



# GRAĐEVINSKI MATERIJALI I KONSTRUKCIJE

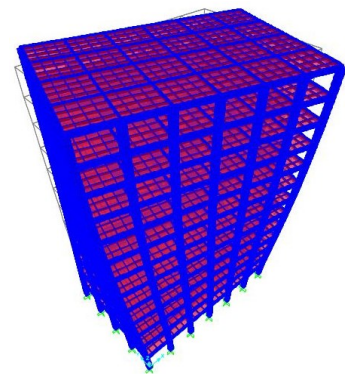
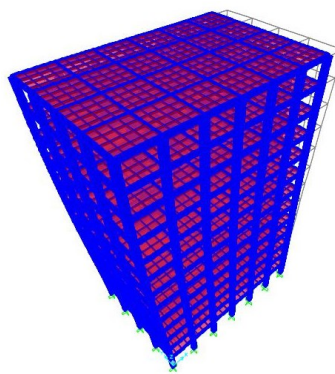
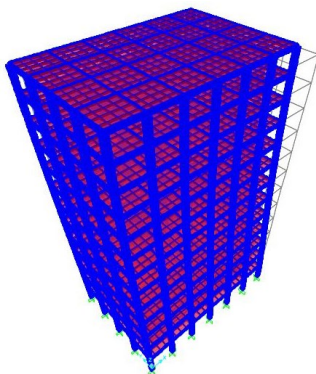
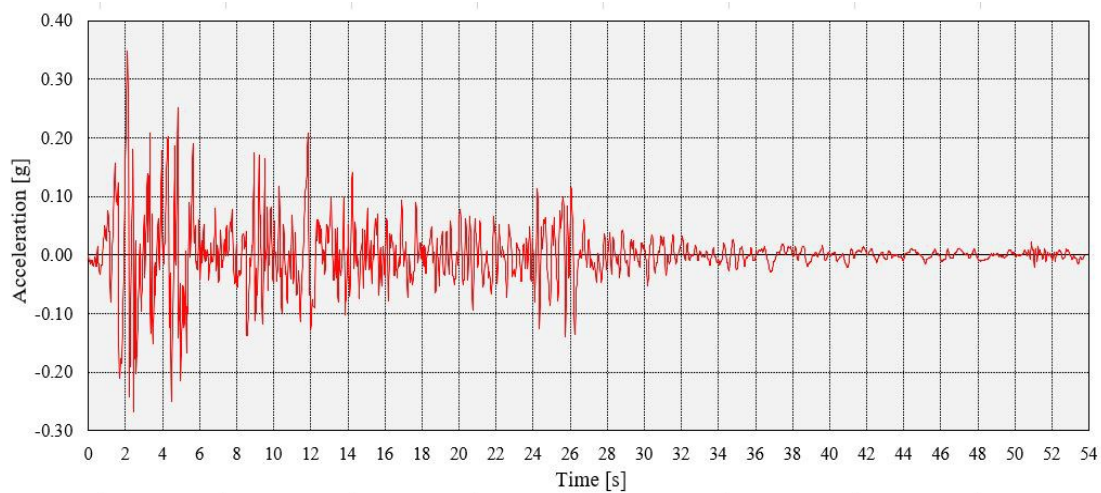
## BUILDING MATERIALS AND STRUCTURES

Volume 65  
June 2022

ISSN 2217-8139 (Print)  
ISSN 2335-0229 (Online)  
UDK: 06.055.2:62-  
03+620.1+624.001.5(49  
7.1)=861

# 2

Society for Materials and Structures Testing of Serbia  
University of Belgrade Faculty of Civil Engineering  
Association of Structural Engineers of Serbia



**CONTENTS**

Borko Miladinović, Slobodan Živaljević, Zvonko Tomanović <b>Influence of material bridges on shear strength of unfilled intermittent rock joints</b> <b>Review paper</b> .....	49
Sandra Filipović, Snezana Marinković, Dimitrije Zakić <b>Environmental assessment of copper slag aggregate concrete</b> <b>Preliminary report</b> .....	57
Sivapriya Vijayasimhan, Jijo James, Yuvaraj Karunanithi, Sushritha Gunipati <b>Durability performance of a lime stabilized expansive soil with egg shell ash as a subsidiary admixture</b> <b>Preliminary report</b> .....	65
Andrija Zorić, Dragan Zlatkov, Marina Trajković-Milenković, Todor Vacev, Žarko Petrović <b>Analysis of the seismic response of an RC frame structure with lead rubber bearings</b> <b>Technical paper</b> .....	73
Instructions for authors .....	81

**EDITORIAL BOARD**

**Editor-in-Chief**

Professor **Snežana Marinković**  
University of Belgrade, Faculty of Civil Engineering, Institute  
for Materials and Structures, Belgrade, Serbia  
e-mail: [sneska@imk.grf.bg.ac.rs](mailto:sneska@imk.grf.bg.ac.rs)

**Deputy Editor-in-Chief**

Professor **Mirjana Malešev**  
University of Novi Sad, Faculty of Technical Sciences,  
Department of Civil Engineering, Novi Sad, Serbia  
e-mail: [miram@uns.ac.rs](mailto:miram@uns.ac.rs)

**Members**

Professor **Jose M. Adam**  
ICITECH, Universitat Politècnica de Valencia, Valencia,  
Spain

Dr **Ksenija Janković**  
Institute for Testing Materials – Institute IMS, Belgrade,  
Serbia

Professor Emerita **Dubravka Bjegović**  
University of Zagreb, Faculty of Civil Engineering,  
Department of materials, Zagreb, Croatia

Professor Academician **Yatchko P. Ivanov**  
Bulgarian Academy of Sciences, Institute of Mechanics,  
Sofia, Bulgaria

Professor **Tatjana Isaković**  
University of Ljubljana, Faculty of Civil and Geodetic  
Engineering, Ljubljana, Slovenia

Professor **Michael Forde**  
University of Edinburgh, Institute for Infrastructure and  
Environment, School of Engineering, Edinburgh, United  
Kingdom

Professor **Vlastimir Radonjanin**  
University of Novi Sad, Faculty of Technical Sciences,  
Department of Civil Engineering, Novi Sad, Serbia

**Predrag L. Popovic**  
Vice President, Wiss, Janney, Elstner Associates, Inc.,  
Northbrook, Illinois, USA

Professor **Zlatko Marković**  
University of Belgrade, Faculty of Civil Engineering,  
Institute for Materials and Structures, Belgrade, Serbia

Professor **Vladan Kuzmanović**  
University of Belgrade, Faculty of Civil Engineering,  
Belgrade, Serbia

Professor Emeritus **Valeriu A. Stoian**  
University Politehnica of Timisoara, Department of Civil  
Engineering, Research Center for Construction  
Rehabilitation, Timisoara, Romania

Secretary:

**Slavica Živković**, Master of Economics  
Society for Materials and Structures Testing of Serbia, 11000 Belgrade, Kneza Milosa 9  
Telephone: 381 11/3242-589; e-mail: [office@dimk.rs](mailto:office@dimk.rs), web sajt: [www.dimk.rs](http://www.dimk.rs)

English editing:

Professor **Jelisaveta Šafranč**, University of Novi Sad, Faculty of Technical Sciences, Novi Sad, Serbia

Technical support:

**Stoja Todorović**, e-mail: [saska@imk.grf.bg.ac.rs](mailto:saska@imk.grf.bg.ac.rs)

Dr **Vilma Ducman**  
Head of Laboratory for Cements, Mortars and  
Ceramics, Slovenian National Building and Civil  
Engineering Institute, Ljubljana, Slovenia

Assistant Professor **Ildiko Merta**  
TU Wien, Faculty of Civil Engineering, Institute of  
Material Technology, Building Physics, and Building  
Ecology, Vienna, Austria

Associate Professor **Ivan Ignjatović**  
University of Belgrade, Faculty of Civil Engineering,  
Institute for Materials and Structures, Belgrade, Serbia

Professor **Meri Cvetkovska**  
University "St. Kiril and Metodij", Faculty of Civil  
Engineering, Skopje, Macedonia

Dr **Anamaria Feier**  
University Politehnica of Timisoara, Department for  
Materials and Manufacturing Engineering, Timisoara,  
Romania

Associate Professor **Jelena Dobrić**  
University of Belgrade, Faculty of Civil Engineering,  
Institute for Materials and Structures, Belgrade, Serbia

Dr **Vladimir Gocevski**  
Hydro-Quebec, Mécanique, structures et architecture,  
Ingénierie de production, Montréal (Québec), Canada

Dr **Nikola Tošić**  
MSCA Individual Fellow, Civil and Environmental  
Engineering Department, Universitat Politècnica de  
Catalunya (UPC), Barcelona, Spain

Assistant Professor **Ehsan Noroozinejad Farsangi**  
Earthquake Engineering Department, Graduate  
University of Advanced Technology, Iran

## Aims and scope

Building Materials and Structures aims at providing an international forum for communication and dissemination of innovative research and application in the field of building materials and structures. Journal publishes papers on the characterization of building materials properties, their technologies and modeling. In the area of structural engineering Journal publishes papers dealing with new developments in application of structural mechanics principles and digital technologies for the analysis and design of structures, as well as on the application and skillful use of novel building materials and technologies.

The scope of Building Materials and Structures encompasses, but is not restricted to, the following areas: conventional and non-conventional building materials, recycled materials, smart materials such as nanomaterials and bio-inspired materials, infrastructure engineering, earthquake engineering, wind engineering, fire engineering, blast engineering, structural reliability and integrity, life cycle assessment, structural optimization, structural health monitoring, digital design methods, data-driven analysis methods, experimental methods, performance-based design, innovative construction technologies, and value engineering.

<b>Publishers</b>	Society for Materials and Structures Testing of Serbia, Belgrade, Serbia, veb sajt: <a href="http://www.dimk.rs">www.dimk.rs</a> University of Belgrade Faculty of Civil Engineering, Belgrade, Serbia, <a href="http://www.grf.bg.ac.rs">www.grf.bg.ac.rs</a> Association of Structural Engineers of Serbia, Belgrade, Serbia, <a href="http://dgks.grf.bg.ac.rs">dgks.grf.bg.ac.rs</a>
<b>Print</b>	Razvojno istraživački centar grafičkog inženjerstva, Belgrade, Serbia
<b>Edition</b>	quarterly
<b>Peer reviewed journal</b>	
<b>Journal homepage</b>	<a href="http://www.dimk.rs">www.dimk.rs</a>
<b>Cover</b>	<b>Accelerogram of Imperial Valley earthquake, component north-south (up), The first three mode shapes and natural periods of the rigidly founded structure (down)</b> , from <i>Analysis of the seismic response of an RC frame structure with lead rubber bearings</i> by Andrija Zorić, Dragan Zlatkov, Marina Trajković-Milenković, Todor Vacev and Žarko Petrović
<b>Financial support</b>	Ministry of Education, Science and Technological Development of Republic of Serbia University of Belgrade Faculty of Civil Engineering Institute for testing of materials-IMS Institute, Belgrade Faculty of Technical Sciences, University of Novi Sad, Department of Civil Engineering Serbian Chamber of Engineers

CIP - Каталогизacija y publikaciji  
Narodna biblioteka Srbije, Beograd

620.1

**GRAĐEVINSKI materijali i konstrukcije** = Building materials and structures / editor-in-chief Snežana Marinković  
. - God. 54, br. 3 (2011)- . - Belgrade : Society for Materials and Structures Testing of Serbia : University of Belgrade, Faculty of Civil Engineering : Association of Structural Engineers of Serbia, 2011- (Belgrade : Razvojno istraživački centar grafičkog inženjerstva). - 30 cm

Tromesečno. - Je nastavak: Materijali i konstrukcije  
= ISSN 0543-0798. - Drugo izdanje na drugom medijumu:  
Građevinski materijali i konstrukcije (Online) = ISSN 2335-0229  
ISSN 2217-8139 = Građevinski materijali i konstrukcije  
COBISS.SR-ID 188695820



## Influence of material bridges on shear strength of unfilled intermittent rock joints

Borko Miladinović<sup>\*1)</sup>, Slobodan Živaljević<sup>1)</sup>, Zvonko Tomanović<sup>2)</sup><sup>1)</sup> University of Montenegro, Faculty of Civil Engineering, George Washington St, 81000 Podgorica, Montenegro<sup>2)</sup> GeoT d.o.o. Podgorica, Đoka Miraševića br. 6, Podgorica, Montenegro

### Article history

Received: 09 April 2022

Received in revised form:

16 May 2022

Accepted: 24 May 2022

Available online: 30 June 2022

### Keywords

Intermittent rock joints,  
material bridge,  
shear strength,  
CNS direct shear test

### ABSTRACT

According to the well-known Jaeger's theory, the minimum possible rock mass shear strength as a discontinuum actually corresponds to the shear strength of rock joints. Since failures in rock masses due to loads caused by civil structures or civil works occur mainly by exceeding their shear strength, the shear strength of rock joints has huge practical significance. Therefore, in this paper it was decided to analyse a factor which can have a very important influence on the shear strength of unfilled rock joints. Namely, the influence of the presence of material bridges and initial joints between them, their number, size, mutual distance and orientation relative to the shearing direction were analyzed using results of laboratory or numerical CNS direct shear tests which were carried out by different researchers around the world. Except for increasing its peak and residual value, the professional public is currently unaware of the impact of this factor on the shear strength of intermittent rock joints. Based on the carried out analysis, appropriate conclusions have been made.

## 1 Introduction

The single plane of weakness theory proposed by Jaeger is the most widely known in Rock Mechanics. According to Jaeger's theory, the minimum possible rock mass shear strength as a discontinuum actually corresponds to the shear strength of rock joints (discontinuities). Since failures in rock masses due to loads caused by civil structures or civil works occur mainly by exceeding their shear strength, the shear strength of rock joints has huge practical significance in Rock engineering, especially in Rockslide and slope engineering. Therefore, in this paper it was decided to analyse the factor which has a very important influence on the shear strength of unfilled rock joints and their mechanical behaviour during shearing. Namely, after a short analysis of the influence of well-known factors such as joint surface roughness and rock compressive strength at the joint surface, special attention is paid to the influence of the presence of material bridges and initial joints between them, their number, size, mutual distance, and orientation relative to the shearing direction.

## 2 Mechanical behaviour of unfilled rock joints during shearing

A number of factors influence the mechanical behaviour of natural unfilled rock joints during shearing, including joint surface roughness (roughness of the joint walls), the presence of material bridges and their configuration, rock compressive strength at the joint surface (compressive

strength of the joint walls), the level of normal stress during shearing  $\sigma_n$ , and the scale effect. These factors will be analyzed in more detail below.

### 2.1 Joint surface roughness

A planar, smooth, and clean natural rock joint is very rare. All natural rock joint surfaces exhibit some degree of roughness, varying from smoothed and polished sheared rock joints with very low surface roughness to very rough tension rock joints. This degree of roughness has a significant effect on the shear strength of unfilled rock joints. This effect can be quantitative or qualitative in nature. Quantitative means that joint surface roughness often increases the peak shear strength of rock joint  $\tau_p$  well above the minimum value of shear strength [1, 2]. This minimum shear strength is defined by the basic friction angle  $\phi_b$  and its characteristic for planar, smooth, and clean unfilled rock joints (Fig. 1). Qualitative means that joint surface roughness can cause a change in the type of mechanical behaviour of unfilled joints during shearing. It is quite clear if we compare the shear stress  $\tau$  vs. shear displacement  $\delta$  curves (hereinafter shear curves) for planar, smooth and unfilled rock joints in granite Hwangdeung recorded by Jang et al. [3] in the CNS direct shear test (Fig. 2) with normalized shear stress  $\tau/\sigma_n$  vs. shear displacement  $\delta$  curves (hereinafter normalized shear curves) for natural joints in different rocks recorded by Grasselli [1] also in the CNS direct shear test (Fig. 3).

<sup>\*</sup> Corresponding author:E-mail address: [borkom@ucg.ac.me](mailto:borkom@ucg.ac.me)

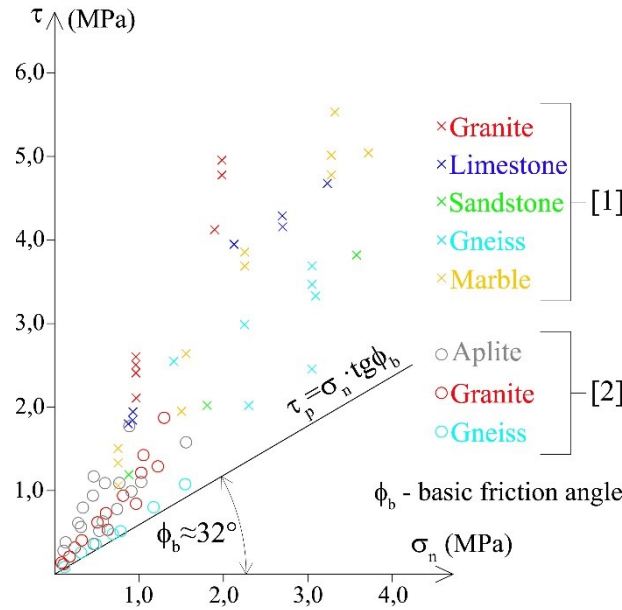


Figure 1. Values of peak shear strength for natural unfilled rock joints in different rocks with  $\phi_b \approx 32^\circ$  which are measured in CNS direct shear test. Adapted from [1, 2]

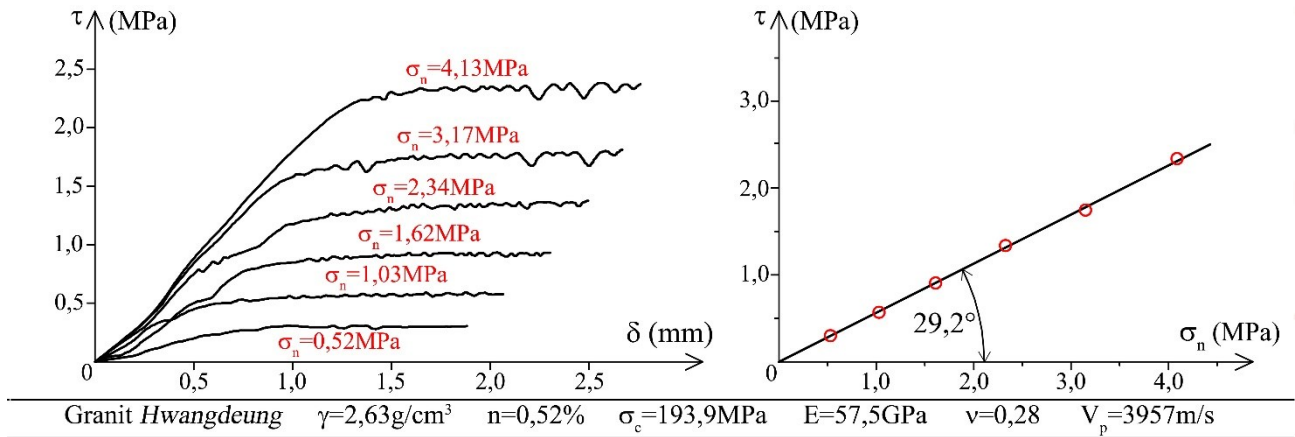


Figure 2. Results of CNS direct shear tests with different values of normal stress during shearing for planar, smooth and unfilled rock joints in granite Hwangdeung. Left: shear curves. Right: linear MC failure envelope. Adapted from [3]

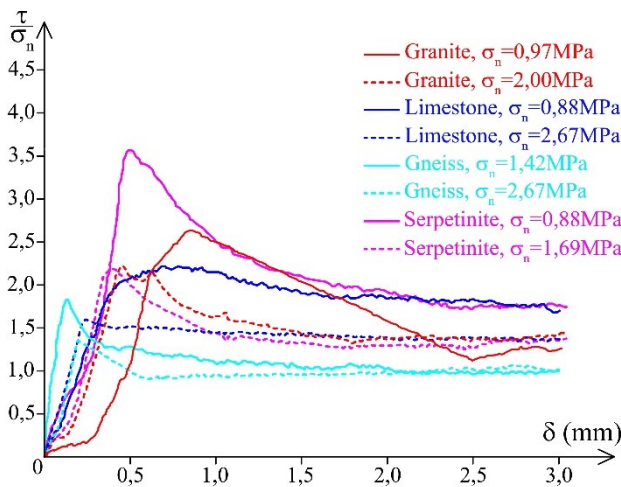


Figure 3. Normalized shear curves for nature unfilled rock joints in different rocks recorded in CNS direct shear tests with different values of normal stress during shearing. Adapted from [1]

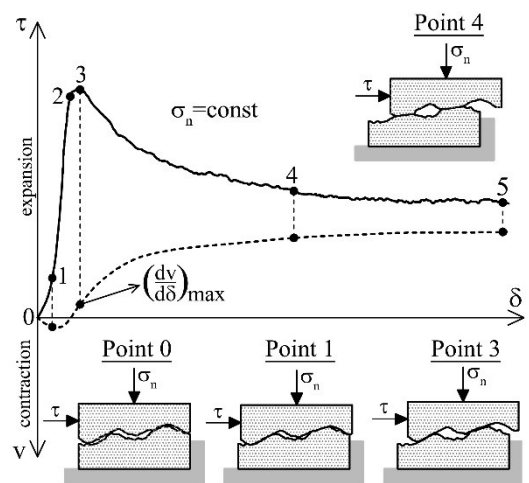


Figure 4. Typical shear curves and dilation curves for nature unfilled rock joints recorded in CNS direct shear test. Adapted from [2]

Fig. 4 shows a typical shear stress  $\tau$  vs. shear displacement  $\delta$  and vertical displacement  $v$  vs. shear displacement  $\delta$  curves (dilation curves) for natural unfilled rock joints recorded in CNS direct shear tests. In general, it can be concluded that the peak shear strength of natural unfilled rock joints (unfilled rock joints with a greater or lesser degree of surface roughness) can be considered a function of three variables: normal stress  $\sigma_n$ , basic friction angle  $\phi_b$  and peak dilation angle  $\psi_{max}$ . Unlike the basic friction angle, which can be considered constant for the analyzed rock type, the peak dilation angle  $\psi_{max}$  is not constant. The value of this angle depends on the level of normal stress  $\sigma_n$  during shearing as well as the joint surface roughness, the presence of material bridges and their configuration, and rock compressive strength at the joint surface. Also, the peak dilation angle is scale dependent, i.e., the peak dilation angle, as well as the peak shear strength of natural unfilled rock joints, depends on the scale effect.

## 2.2 Rock compressive strength of the joint surface

Numerous experimental studies of natural unfilled rock joints have clearly shown that their shear strength depends on the rock compressive strength at the joint surface, i.e., the compressive strength of the bumps, ripples, and undulations on the rock joint surface (joint walls). These surface irregularities are given the general term asperities. The strength of the asperities is extremely important because they represent the sites (locations, points) of a stress concentration during shearing. The well-known effects of dilation and the effect of interlocking, which increase the shear strength of rock joints, occur (are pronounced) when asperities have more significant strength. In this case, the shearing process takes place over the asperity surface. However, if the strength of the asperities is lower, during shearing the asperities progressively shear off. In that case, the shearing process takes place through the asperities. For that reason, previously mentioned effects either do not exist or are very weakly expressed, which negatively affects the shear strength of rock joints.

The rock compressive strength of the joint surface can be equal to the compressive strength of intact rock. This may be the case with completely closed rock joints, and then one can talk about a fresh joint surface. However, due to the effects of weathering rock, the compressive strength of the joint surface is usually significantly less than the compressive strength of intact rock. Then one can talk about the weathered joint surface.

## 2.3 Level of normal stress during shearing

It is totally clear that the increase in normal stress  $\sigma_n$  causes an increase in the shear strength of rock joints. Shear tests carried out on planar, smooth, and clean unfilled rock joints under constant normal stress generally give a constant value of the ratio  $\tau_p/\sigma_n$ , which is actually equal to  $\tan \phi_b$  at any level of normal stress. However, for naturally unfilled rock joints with a greater or lesser degree of joint surface roughness, the ratio  $\tau_p/\sigma_n$  is not constant. The value of the peak friction angle of the joint surface  $\phi_p$ , which actually represents the sum of the basic friction angle  $\phi_b$  and peak dilation angle  $\psi_{max}$ , depends on the level of normal stress during shearing. The value of the peak dilation angle  $\psi_{max}$ , as well as the value of the peak friction angle of the joint surface  $\phi_p$ , decreases with the increasing value of normal stress  $\sigma_n$ . Thus, with increasing normal stress during

shearing, the peak friction angle of the joint surface  $\phi_p$  tends to the value of the basic friction angle  $\phi_b$ . Since the dilation is a direct consequence of the joint surface roughness, it means that the influence of this roughness on the shear strength of the rock joint is significant but at lower values of the normal stress  $\sigma_n$ . At higher values of normal stress, degradation or complete crushing of asperities occurs, which negatively affects the value of the peak dilation angle. All of the above directly leads to the conclusion that the failure envelope for natural, unfilled rock joints (to a varying degrees of joint surface roughness) is nonlinear.

When analyzing the influence of normal stress on the shear strength of natural unfilled rock joints (to a greater or lesser degree of joint surface roughness), it is useful to mention the effect of "pre-stress". Actually, this effect is identical to the well-known effect of soil pre-consolidation. The shear strength of any natural unfilled rock joints depends on the value of the normal stress  $\sigma_n$  during shearing. However, the value of the shear strength of the joint can also be significantly affected by whether the normal stress  $\sigma_n$  is at the same time the highest normal stress that has ever acted on this rock joint. In general, an increase in the value of the "pre-stress" coefficient leads to an increase in the value of the shear strength of rock joints.

## 2.4 Scale effect

The value of the peak friction angle of the joint surface  $\phi_p$  represents the sum of the basic friction angle  $\phi_b$  and the peak dilation angle  $\psi_{max}$ . Bandis [4] divided the peak dilation angle into two components. The first component, known as the geometrical asperity component, represents the average slope of the dominant (main) asperities on the joint walls relative to the shear direction. The second component, known as the mechanical asperity component, represents the strength of the dominant (main) asperities on the joint walls. According to the results of the carried out CNS direct shear tests, Bandis [4] concluded that the values of both components of the peak dilation angle decrease with the increasing dimensions of the examined rock joint, i.e., dimensions of the examined rock specimen with joint (scale effect). It is important to note that the basic friction angle  $\phi_b$  is one of the few parameters in Rock Mechanics that does not depend on the scale effect. Shear tests carried out on planar, smooth, and clean unfilled rock joints of different dimensions under constant normal stress generally give a constant value of the ratio  $\tau_p/\sigma_n$ , which is actually equal to  $\tan \phi_b$ .

## 3 Mechanical behaviour of unfilled intermittent rock joints during shearing

The discontinuity of natural unfilled rock joints by material bridges or some healed sections may have a significant influence on their shear strength. It is totally clear that the presence of material bridges increases the shear strength of rock joints in proportion to the material bridge ratio  $\xi_b$  (material bridge area divided by total joint surface area). Except for the ratio  $\xi_b$  and configuration of material bridges also may have very significant influence on the shear strength of intermittent rock joints. The configuration of material bridges implies their shape, number, size, mutual distance, and orientation relative to the shear direction.

The mechanical behaviour of intermittent rock joints during shearing is very complicated and insufficiently investigated. So far, this type of mechanical behaviour has

been commonly investigated in direct shear tests carried out on specimens of rock-like material (for example, gypsum) with intermittent joints which are easily formed during the pouring of the specimens. If specimens of intact rock material are used in direct shear tests, the intermittent joints are formed by cutting the specimens in a controlled manner (in certain zones and at a certain angle) with a diamond tile saw. Also, for the analysis of the mechanical behaviour of intermittent rock joints during shearing, numerical simulations of direct shear tests were performed by different researchers using sophisticated software.

Probably one of the most extensive and significant experimental investigations of the mechanical behaviour of unfilled intermittent rock joints during shearing was performed by German engineers Gehle and Kutter [5] from Rohr-University. They prepared more than 130 prism-shaped specimens with intermittent joints and tested them in the CNS displacement-controlled direct shear test ( $\sigma_n=1.0\text{MPa}$ ,  $v=2\text{mm/s}$ ). They analyzed different configurations of material bridges and their influences on the mechanical behaviour of joints during shearing (Fig. 5). The majority of the specimens tested were made from a gypsum + water mixture that was poured into a steel mould with internal dimensions of  $B/L/H=5\text{cm}/25\text{cm}/15\text{cm}$ . The rest of the tested specimens consisted of natural specimens of limestone with the same dimensions as gypsum (artificial) specimens. Shear (horizontal) displacement  $\delta$  was applied to all tested specimens at a same controlled speed, and the values of generated shear stress  $\tau$  and vertical displacement  $v$  were recorded. Fig. 6 shows results which Gehle and Kutter [5] recorded in two selected direct shear tests, i.e., for two selected artificial specimens.

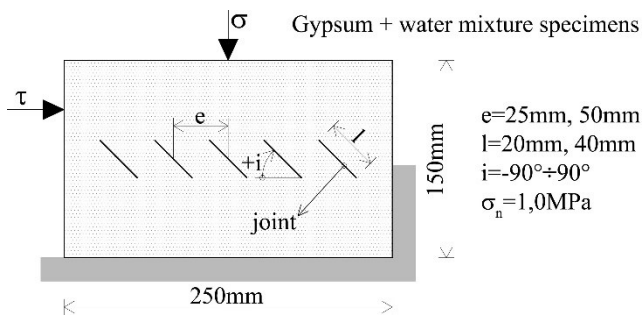


Figure 5. Geometrical characteristics of used specimens with intermittent joints. Adapted from [5]

First of all, according to the presented results, it can be concluded that the mechanical behaviour of an unfilled intermittent rock joint during shearing is very complicated. In the initial phase of the test, the increase in shear displacement  $\delta$  is followed by an intense increase in shear stress  $\tau$ . With some minor deviations, it can be considered that the shear stress is linearly related to shear displacement. The proportionality of this relationship corresponds to the stiffness of material bridges. At one moment, it comes to a sudden drop in shear stress (shear resistance). At that time, the initial joints are completely interconnected by cracks formed through material bridges. Actually, at that time, continuous (non-intermittent) joints were formed in the tested specimens. The geometric characteristics of the formed continuous joints depend on the configuration of the initial joints and material bridges. With a further increase in the shear displacement, the mechanical behaviour of the tested joints corresponds to the mechanical behaviour of rock joints with a greater or lesser degree of

surface roughness during shearing. In this phase of the test, dilation is very pronounced.

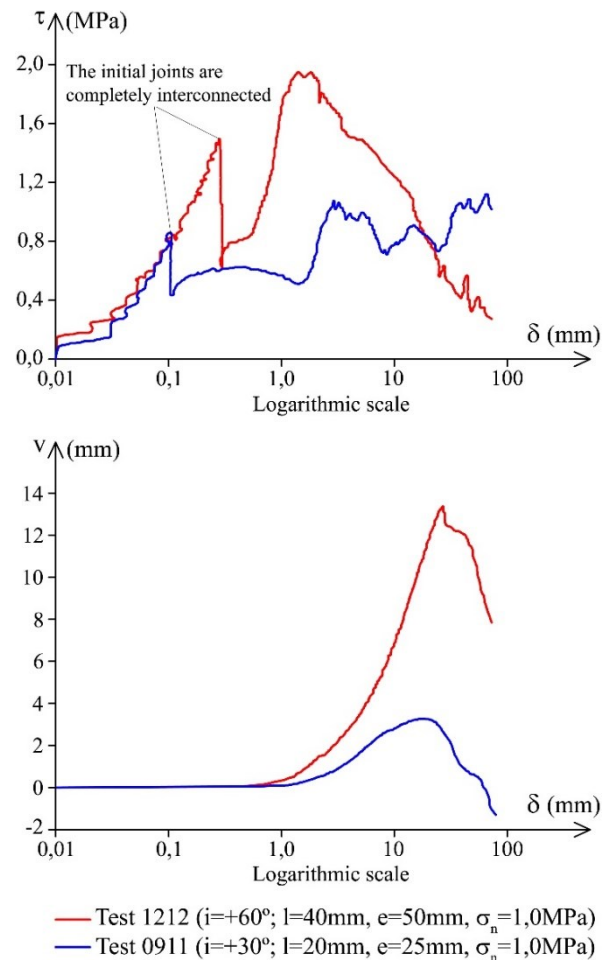


Figure 6. Examples of results of two different tests ( $\sigma_n=1\text{MPa}$ ). Above: shear. Below: dilation curves. Adapted from [5]

It can be seen from Fig. 6 that a large horizontal displacement  $u_{max}=65\text{mm}$  is applied to the tested specimens. This displacement is actually 26% of the length of the shear plane and it is significantly larger than the initial distance between the individual joints. However, in both cases, the residual shear strength of the intermittent joints was not reached. For example, Grasselli [1] recorded that the shear displacements of approximately 3% of the shear plane length were sufficient to generate residual shear strength of the unfilled rock joints with pronounced joint surface roughness. Gehle and Kutter [5] claim that the shear displacement of 65mm is sufficient to record all of the significant shear behaviour characteristics for tested specimens.

Summarizing the results of the performed investigations, Gehle and Kutter [5] defined some main principles of the mechanical behaviour of unfilled intermittent rock joints during shearing. As a final result of the research, regardless of the numerous and significant differences in the recorded results of individual experiments, the authors proposed an idealized shear curve that describes the mechanical behaviour of unfilled intermittent rock joints during shearing under constant normal stress (Fig. 7). As can be seen, Gehle and Kutter [5] divide the mechanical behaviour of this type of rock joint during shearing into three phases.

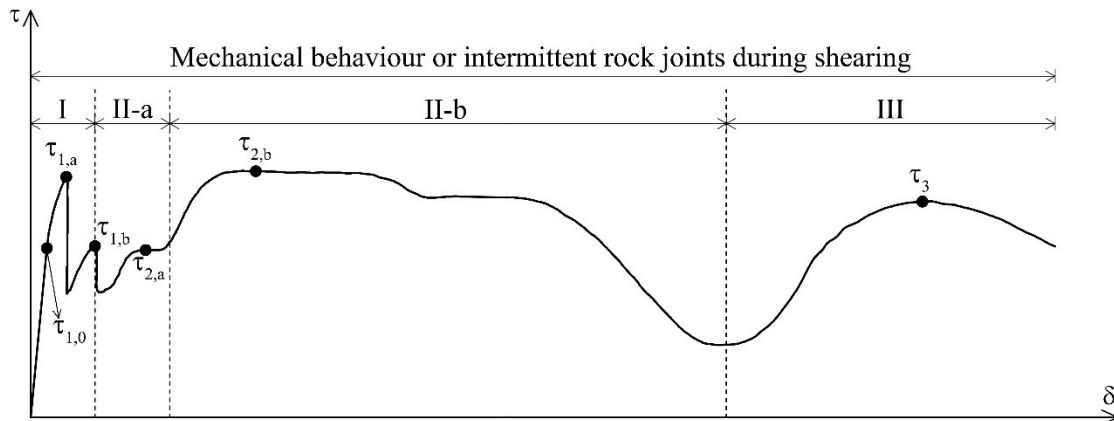


Figure 7. Idealized shear curve for unfilled intermittent joints during shearing under constant normal stress. Adapted from [5]

Since the stiffness of material bridges is many times greater than the stiffness of individual joints, in the first phase the increase in shear displacement causes a concentration of the shear stress on these bridges. Elastic deformations are only recorded, and it can be considered that the measured shear stress  $\tau$  is linearly related to the applied shear displacement  $\delta$ . However, fractures of material bridges occur when the concentrated shear stresses reach the value of the shear strength of material bridges (shear strength of intact rock). Formed cracks pass through the material bridges and connect the initial joints. It is very important to note that these fractures occur successively. The appearance of the first fracture or the first crack passing through any material bridge actually represents the beginning of the nonlinear mechanical behaviour of unfilled intermittent joints during shearing. At that time, the registered value of the shear stress is  $\tau_{1,0}$ . In some specimens at that time, but in most specimens at a slightly higher value of the applied shear displacement (measured shear stress is  $\tau_{1,a}$ ), several cracks have already formed through the material bridges. These cracks lead to a sudden drop in the shear strength of intermittent joints. After that, the shear strength of the joints usually slightly increases until the shear stress  $\tau_{1,b}$  is reached. Then it usually comes to a sudden drop in the shear strength of the joints. This drop actually means that all the initial joints are finally connected.

During the first phase of the shearing, continuous (non-intermittent) joints with more or less a "saw-tooth" surface were formed in the tested (sheared) specimens with  $i \neq 0$ . Between "saw-tooth" joint walls, relatively large cut-out fragments of rock-like (rock) material were trapped. In the tested specimens with  $i = 0$  during the first phase of the shearing, continuous joints with more or less planar and smooth surfaces were formed, which primarily depends on the length and mutual spacing of the initial joints.

After the first phase, in the shearing process of unfilled intermittent joints, the second phase occurs. It lasts much longer, i.e., it covers a significantly larger shear displacement interval compared to the first phase. Generally, the second phase of the shearing process can be divided into two sub-phases. During the first sub-phase (II-a), an intensive increase in dilation angle is recorded. However, it is not followed by an equally intensive and pronounced increase in the shear strength of the tested joints. The reason for this is the small contribution of pure (physical) friction between the "saw-tooth" joint walls and their shear resistance angle. The initial joints are open, so the contact between their walls is realized only indirectly through the cut-out fragments of rock-

like (rock) material. As the shear displacement increases, these cut-out fragments rotate. It is known that the friction during rotation is many times less than during sliding. The maximum measured value of the shear stress in this sub-phase is  $\tau_{2,a}$ .

In the second sub-phase (II-b) of the shearing process, with the increase of shear displacement  $\delta$  direct contact between the "saw-tooth" joint walls is gradually realized. For that reason, the shear strength of tested (sheared) joints usually increases. At the moment of closing the initial joints, the measured value of the shear stress is  $\tau_{2,b}$ . As the shear displacement increases, the dilation stops and the shear resistance is solely based on the friction between the joint walls. The end of the second sub-phase was marked by a sudden drop in the shear strength of tested joints followed by intense contraction of the tested specimens. The contraction is the result of the degradation and crushing of cut-out fragments of rock-like (rock) material that are "trapped" between the joint walls.

Finally, at relatively large values of the applied shear displacement, the third phase of the shearing process occurs. In this phase, the peak shear strength of tested (sheared) joints  $\tau_3$  is predominantly conditioned by the shear resistance angle of degraded and crushed material that fills the space between joint walls, i.e., fills the space of formed shear zones in the sheared specimens. The width of the shear zone primarily depends on the geometric characteristics of the initial joints. It is useful to note that for some sheared specimens, this shear strength was the maximum shear strength that was recorded during the whole shearing process. At this stage, small or negligible changes in the volume of the sheared specimens were registered.

Each of the previously described phases or sub-phases of the mechanical behaviour of unfilled intermittent joints during shearing has its characteristic peak shear strength. It is important to note that each of these so-called phase peak shear strengths (except  $\tau_{1,0}$ ) in some sheared specimens actually represented the maximum measured value of shear strength during shearing under constant normal stress. For example, in all sheared specimens with horizontal initial joints ( $i = 0$ ), the highest measured value of shear strength in the whole shearing process was  $\tau_{1,a}$ . However, in all sheared specimens with vertical initial joints ( $i = 90^\circ$ ), the highest measured value of shear strength in whole shearing process was  $\tau_{2,b}$ . Generally, in the case of sheared specimens with a negative initial joint inclination ( $-90^\circ < i < 0^\circ$ ), the highest measured value of shear strength in the whole shearing

process was  $\tau_{2,a}$ . In sheared specimens with positive initial joint inclination ( $0 < i < 90^\circ$ ) and depending on their mutual distance, the highest measured value of shear strength in whole shearing process was often  $\tau_{2,b}$ , then  $\tau_3$  and rarely  $\tau_{1,a}$ . In general, in the performed direct shear tests under constant normal stress, the highest shear strengths were measured on the specimens with a negative initial joint inclination, which is a consequence of very pronounced dilation in these specimens.

After Gehle and Kutter [5], Zhang et al. [6] carried out significant research on the shear strength of intermittent rock joints. Numerically, using the FE method with the help of appropriate software, he simulated the shear of rock-like specimens with intermittent joints (jointed rock-like specimens) in a CNS displacement-controlled direct shear test ( $\sigma_n = 0,15 \text{ MPa}$ ,  $v = 2 \text{ mm/s}$ ). The stress-strain behaviour of used rock-like material is defined by appropriate constitutive relations for a finite element under uniaxial compressive stress and tensile stress (Fig. 8.). The values of the used mechanical parameters for these constitutive relations are also given in Fig. 8. Two groups of jointed rock-like specimens were tested. In the first group of specimens, all initial joints are horizontal  $i = 0$  (Fig. 8). Their width  $b$  was varied, i.e., the value of material bridge ratio  $\xi_b$  was varied. In the second group of specimens, the total number, width, and mutual distance of initial joints were constant but their slope relative to the shear direction was varied (Fig. 8).

The peak shear strength of the first group of jointed rock-like specimens was found to increase almost linearly with increasing width of initial joints, i.e., with increasing value of material bridge ratio  $\xi_b$ . However, for the second group of jointed rock specimens, measured values of the shear strength are highly non-linearly related to the values of angle  $i$  (Fig. 9). Generally, the peak shear strength of intermittent rock joints in the case of a negative value of angle  $i$  is higher than those in the case of a positive value of angle  $i$ .

Sarfazi and Schubert [7] also carried out experimental research on the mechanical behaviour of unfilled intermittent rock joints during shearing. They prepared two groups of nine prism-shaped rock-like specimens with intermittent joints and tested them in the CNS displacement-controlled direct shear test ( $\sigma_n = 1.0 \text{ MPa}$ ,  $v = 2 \text{ mm/s}$ ). All specimens tested were made from a gypsum + water mixture that was poured into a steel mould with internal dimensions of  $B/L/H = 15 \text{ cm}/15 \text{ cm}/15 \text{ cm}$ . They analyzed different configurations of material bridges and their influences on the mechanical behaviour of joints during shearing. All jointed rock-like specimens had only horizontal initial joints  $i = 0^\circ$ . All jointed rock-like specimens from the same group had an identical value of material bridge ratio  $\xi_b$ . The shape, size, and mutual distance of the horizontal initial joints were varied. Research carried out by Sarfazi and Schubert [7] showed that from the aspect of the shear strength of intermittent rock joints, the best configuration of material bridges is a configuration with a small number of larger material bridges that are elongated in the shear direction.

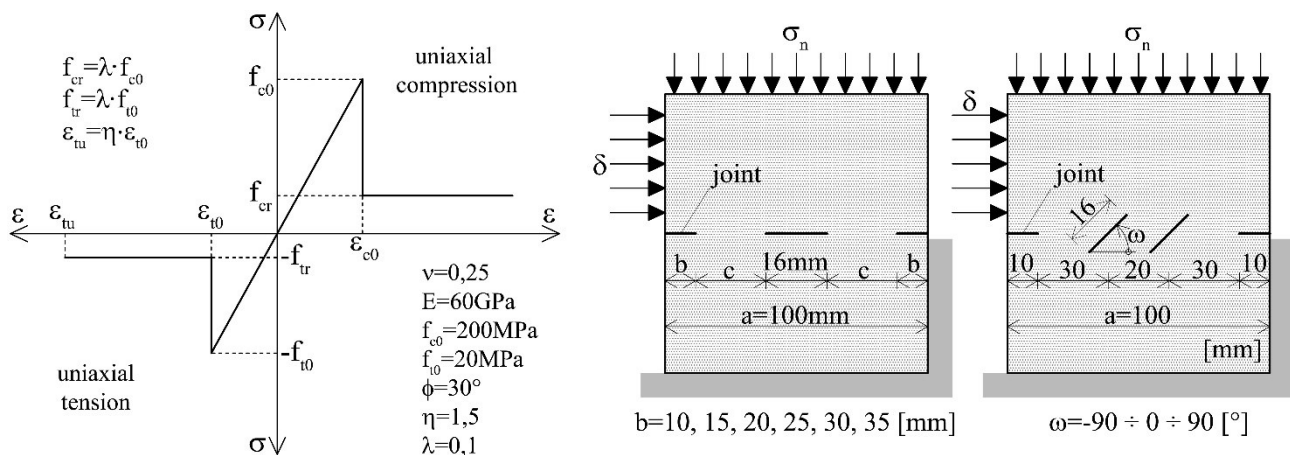


Figure 8. Left: the stress-strain behaviour of used rock-like material. Middle: first group of tested jointed rock-like specimens. Right: second group of tested jointed rock-like specimens. Adapted from [6]

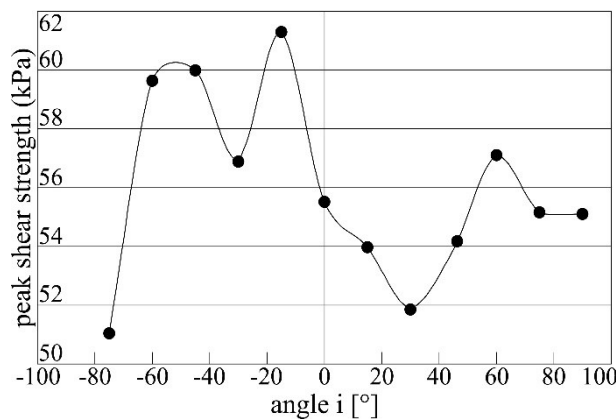


Figure 9. The relationship between peak shear strength of intermittent rock joint and angle  $i$ . Adapted from [6]

Fan et al. [8] also carried out experimental research on the mechanical behaviour of unfilled intermittent rock joints during shearing. They prepared six prism-shaped rock-like specimens with intermittent joints and tested them in the CNS displacement-controlled direct shear test ( $\sigma_n=2.5\text{MPa}$ ,  $v=2\text{mm/s}$ ). All specimens tested were made from a gypsum + water mixture that was poured into a steel mould with internal dimensions of  $B/L/H=15\text{cm}/15\text{cm}/3\text{cm}$ . They analyzed different configurations of material bridges and their influences on the mechanical behaviour of intermittent joints during shearing. Namely, all jointed rock-like specimens had three initial joints of the same length ( $L=20\text{mm}$ ) and the same value of angle  $i$ . This angle was set from  $0^\circ$  to  $150^\circ$  with an interval of  $30^\circ$ . For tested rock-like specimens with horizontal initial joints, a brittle-plastic mechanical behaviour was obtained with a clearly expressed value of the peak and residual shear strength. However, for tested rock-like specimens with inclined initial joints, very complicated mechanical behaviour was obtained (Fig. 10). It

goes through three phases. Three characteristic values of the shear strength of these jointed rock-like specimens are recorded: first peak shear strength, second peak shear strength, and residual shear strength. Between the first and second peak shear strength, a sudden drop in shear strength was registered. This drop occurs when the cracks that pass through the material bridges connect all initial joints, i.e., when a continuous (non-intermittent) joint with more or less "saw-tooth" surface is formed. Further, the shear strength increases from the first to the second peak value because the shear takes place more or less "saw-tooth" joint surface. A new sudden drop in shear strength occurs when the generated contact stresses cause degradation and crushing of main joint asperities. After that, with greater or lesser fluctuations, the shear strength of the rock joint tends to a residual value. To reach this value of shear strength, it was necessary to apply a shear displacement to the tested rock-like specimens, which is approximately 30% of the specimen width.

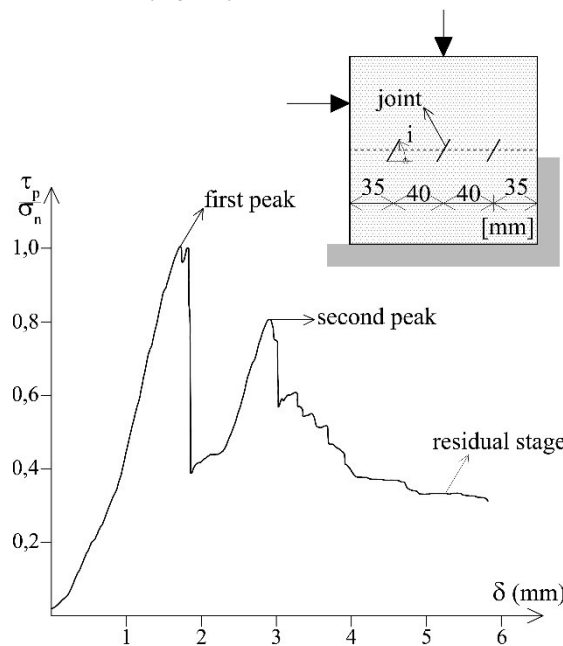


Figure 10. Typical shear curve for jointed rock-like specimens with inclined initial joints. Adapted from [8]

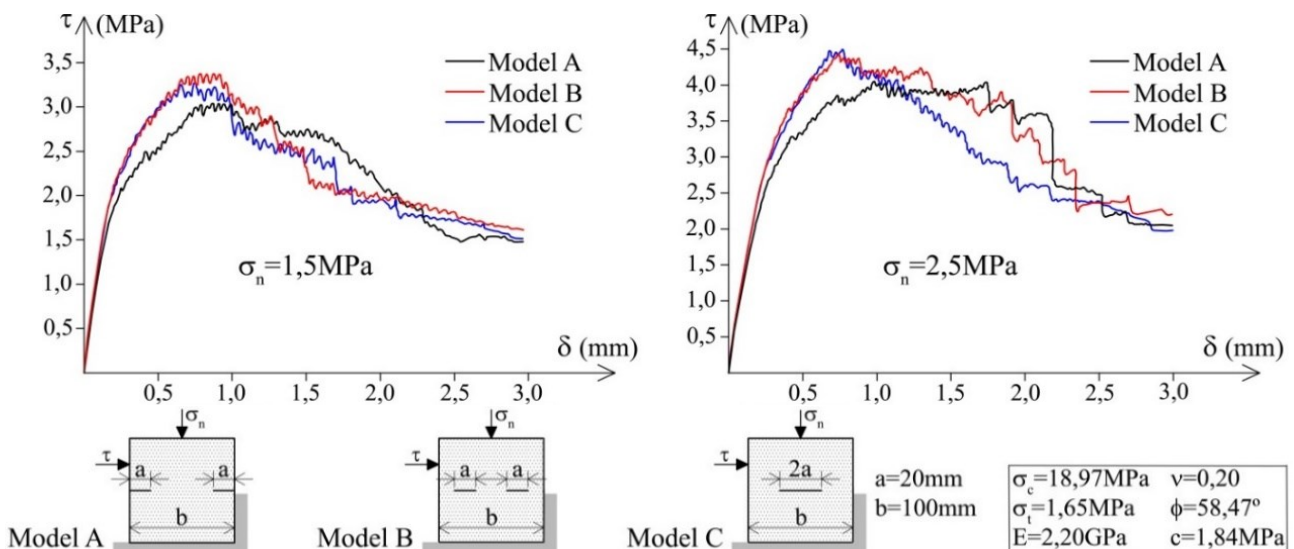


Figure 11. Shear curves for unfilled intermittent rock joints with different configurations of horizontal initial joints. Adapted from [8]

Lin et al. [9] performed a numerical analysis of the mechanical behaviour of unfilled intermittent rock joints during shearing under constant normal stress using the software PFC2D (Particle Flow Code-2D). Intermittent joints with three different configurations of horizontal initial joints (three different models) but with the same value of the material bridge ratio  $\xi_b$  were analyzed. It can be said that for all tested models, it is typically plastic mechanical behaviour with linear-elastic, nonlinear-plastic, peak, strain softening and residual stress phase (Fig. 11). The shear displacement that corresponds to the beginning of the nonlinear-plastic phase increases with an increase in the normal stress. For model C, i.e., for a model with both-side-end initial joints, the lowest value of peak shear strength was recorded. The residual shear strength is achieved at a shear displacement that is approximately 3% of the shear plane length. So, to achieve residual shear strength in the case of intermittent rock joints with horizontal initial joints, it is necessary to apply significantly less shear displacement compared to the case of intermittent rock joints with inclined initial joints.

#### 4 Conclusion

Previously presented research has shown that the mechanical behaviour of unfilled intermittent rock joints during shearing is very complicated. As assumed, it is conditioned by the number, size, shape, mutual distance, and orientation of the material bridges. From the aspect of the shear strength of intermittent rock joints, the best configuration of material bridges is a configuration with a small number of larger material bridges that are elongated in the shear direction. However, the analysis of the results of the previous research came to the conclusion that the slope of the initial joints in relation to the shear direction has a particularly significant influence on the mechanical behavior of the intermittent rock joints.

If the initial joints are horizontal, i.e., parallel to the shear direction, the mechanical behaviour of unfilled intermittent joints during shearing is plastic with linear-elastic, nonlinear-plastic, peak, strain softening and residual stress phase. If the initial joints are inclined, their mechanical behaviour during shearing is very complicated.

This behaviour goes through three phases, and each phase has its own peak shear strength. Which of these three shear strengths will be the largest depends on the orientation and slope of the initial joints in relation to the shear direction. The lowest values of the peak shear strength are obtained

for intermittent rock joints with both-side-end initial joints. To achieve residual shear strength in the case of intermittent rock joints with horizontal initial joints, it is necessary to apply significantly less shear displacement compared to the case of intermittent rock joints with inclined initial joints.

#### References

- [1] G. Grasselli, Shear Strength of Rock Joints Based on Quantified Surface Description. PhD Thesis, Laboratory of Rock Mechanics at the Swiss Federal Institute of Technology, Lausanne, Switzerland, (2001), doi:10.5075/epfl-thesis-2404
- [2] N. Barton, V. Choubey, The Shear Strength of Rock Joints in Theory and Practice, *Rock Mechanics*, 10 (1-2), (1977), pp. 1-54, doi:10.1007/BF01261801
- [3] H.S. Jang, Q.Z. Zhang, S.S. Kang, B.A. Jang, Determination of the Basic Friction Angle of Rock Surfaces by Tilt Tests, *Rock Mechanics and Rock Engineering*, 51, (2017), pp. 989-1004, doi:10.1007/s00603-017-1388-7
- [4] S. Bandis, Experimental Studies of Scale Effects on Shear Strength and Deformation of Rock Joints. PhD Thesis, Department of Earth Sciences, The University of Leeds, (1980)
- [5] C. Gehle, H.K. Kutter, Breakage and Shear Behaviour of Intermittent Rock Joints, *International Journal of Rock Mechanics & Mining Sciences*, 40, (2003), pp. 687-700, doi:10.1016/S1365-1609(03)00060-1
- [6] H.Q. Zhang, Z.Y. Zhao, C.A. Tang, L. Song, Numerical Study of Shear Behaviour of Intermittent Rock Joints with Different Geometrical Parameters, *International Journal of Rock Mechanics & Mining Sciences*, 43, (2006), pp.802-816, doi:10.1016/j.ijrmms.2005.12.006
- [7] V. Sarfarazi, W. Schubert, Sliding Phenomena in Intermittent Rock Joint, *Periodica Polytechnica Civil Engineering*, 61(3), (2017), pp. 351-360, doi:10.3311/PPci.9466
- [8] X. Fan, L. Kaihui, L. Hongpeng, Z. Qihua, S. Zhenhua, Experimental and Numerical Study of the Failure Behaviour of Intermittent Rock Joints Subjected to Direct Shear Load, *Advances in Civil Engineering*, vol. 2018, (2018), pp. 1-19, doi:10.1155/2018/4294501
- [9] H. Lin, X. Ding, R. Yong, W. Xu, S. Du, Effect of Non-persistent Joints Distribution on Shear Behaviour, *Computes Rendus Mecanique*, 347, (2019), pp. 477-489, doi:10.1016/j.crme.2019.05.001



## Preliminary report

## Environmental assessment of copper slag aggregate concrete

Sandra Filipović<sup>\*1)</sup>, Snezana Marinković<sup>2)</sup>, Dimitrije Zakić<sup>2)</sup><sup>1)</sup> Mining and Metallurgy Institute Bor, 19210 Bor, Serbia<sup>2)</sup> University of Belgrade, Faculty of Civil Engineering, Department for Materials and Structures, Bulevar kralja Aleksandra 73, 11000 Belgrade, Serbia

## Article history

Received: 26 April 2022

Received in revised form:

19 May 2022

Accepted: 27 May 2022

Available online: 30 June 2022

## Keywords

concrete,  
copper slag aggregate,  
Life Cycle Assessment,  
environmental impact

## ABSTRACT

Due to the extremely large global production and utilization of concrete, the concrete industry is considered a large consumer of energy and natural resources and one of the main sources of greenhouse emissions and waste generation. Reducing its impacts on the environment is one of the most important paths toward sustainable construction development. Replacing cement and natural aggregates with by-products and waste from other industries is one possible way of achieving this goal. On the other hand, the disposal of industrial waste, which arises from the pyrometallurgical process of copper production, presents a significant environmental load in many developed countries. Research performed so far has shown that concrete made with aggregate obtained from copper slag instead of natural aggregate can be produced with good physical-mechanical properties for various applications. In this work, a cradle-to-gate Life Cycle Assessment of several concrete mixtures where part of the coarse natural aggregate was replaced with copper slag aggregate was performed. The conducted case study was based on Serbian LCI data and local conditions in the vicinity of the town of Bor in Serbia. Results showed that such concrete mixtures can bring environmental benefits regarding natural aggregate preservation and waste reduction if the transport distance of copper slag aggregates is smaller than 20 km. Therefore, from the environmental protection point-of-view, local application of such concrete is recommended.

## 1 Introduction

Concrete is the most commonly used construction material in the world with an average annual global production of about three tons per capita, or a total average production of about  $25 \times 10^9$  tons per year [1], due to its durability and great possibilities of application, simplicity of production, and availability of raw materials [2]. Aggregates occupy between 55% - 80% of the volume of concrete [3]. Natural aggregates (NA) refer to the product of crushed stone produced in quarries, or extracted gravel and sand from the riverbed. However, many countries have a problem with a deficiency of quality sand on the one hand, and growing environmental problems on the other. An example of this is the fact that the current rate of extraction of NA can cover only 9% of the total annual needs in China [4]. On the other hand, the production of primary products in different industrial activities results in various by-products that have almost no practical industrial application. These industrial by-products, which are generated in high quantities worldwide, present serious challenges regarding their disposal [5]. As a result, more ecologically suitable alternatives for their utilization must be found.

Industrial waste, which arises from the pyrometallurgical process of copper production, is one of the most significant

environmental problems in many developed countries. It is estimated that for every ton of produced copper, about 2.2 - 3.0 tons of slag are generated. Approximately 40 million tons of slag are generated from copper production in the world each year [6]. The frightening data on the annual volume of dumped waste material is cause for worldwide worry, and a solution to the problem must be required in accordance with generally acknowledged principles of sustainable development. One possible solution is the use of copper slag aggregates (CSA) as a replacement for NA in concrete [7].

In pyrometallurgical copper processing, different types of slag are produced: smelter slag, converter slag, anode furnace slag, electric and flash furnace slag, etc. Most of these slags, especially those with higher copper content, are recycled by re-entering the process. The concentration of copper in smelter slag usually ranges from 0.5-2.0% (0.3-1.0% from flame furnaces and over 1% from the flash furnace), while converter slag can contain 2-10% of copper.

Slag with copper ore content below 1% has traditionally been considered solid waste and has been disposed of at landfill. This kind of slag has become a significant secondary raw material [8]. One solution to the problems of industrial waste disposal is the application of copper slag in construction. Due to favorable physical-mechanical and chemical characteristics of copper slag, such as low water

\* Corresponding author:

E-mail address: [filipovic@irnbor.co.rs](mailto:filipovic@irnbor.co.rs)

absorption (water absorption of aggregate ( $WA_{24}$ ) 0.6%), high particle density (apparent particle density ( $\rho_{rd}$ ) 3.33  $Mg/m^3$ ), good resistance to crushing (resistance to degradation (LA) 10%) and wear (resistance to wear (micro-Deval) in a wet state ( $M_{DE}$ ) 4%), its use is possible in the production of building materials [9]. Copper slag in building materials has the potential to increase mechanical properties while also lowering costs and easing disposal issues [10].

A large number of studies have been performed on the application of copper slag in concrete: as a substitute for cement, i.e. in the production of cement clinker [11, 12], and as partial or complete substitutes for coarse and fine fractions of NA in concrete mixtures and cement mortars [13, 14]. Previous studies have shown that around 40% replacement of NA with CSA gives a concrete mixture with better properties such as compressive strength, density, workability, durability, or flexural strength in concrete [15]. Tests have shown, for instance, that the optimal use of CSA for replacing fine fractions of NA (grains 0-2 mm) is 40% [16]. Such concretes have good workability, and higher compressive and tensile strengths, but due to the lower water absorption of the aggregate from copper slag, care must be taken when choosing a water-to-cement ratio ( $w/c$ ) [17]. The lower number of tests was related to the physical-mechanical properties of concrete with partial replacement of coarse fractions of NA with CSA [18, 19]. Insufficient results of research into the material itself is the reason for the poor use of concrete with CSA as a substitute for coarse fractions of NA. It could give a clearer picture of the mechanism that takes place during the hardening process and enable the development of generally accepted design principles.

The industrial processing of smelting slag within the Mining and Smelting Basin Bor (RTB "Bor") has been carried out in the Bor Flotation Plant since 2001. Copper slag has been deposited in the immediate vicinity of processing facilities, in the amount of  $16 - 18 \times 10^6$  t, which was the incentive for testing the possibility of replacing NA with CSA in concrete. The process for obtaining the copper slag generally consists of two-stage crushing and separation according to Figure 1. Due to its high hardness, crushing of copper slag results in high electricity consumption and high damage to the crushers used in this process. For that

reason, naturally granulated copper slag from that landfill was used for testing. Considering that in the natural deposited state of copper slag at RTB "Bor", about 70% of deposited material belongs to the 8/16 and 16 / 31.5 mm fractions, testing was performed on concrete mixtures where part of these fractions of NA was replaced with CSA.

## 2 Mechanical and durability related properties of CSAC – own investigation

Concrete with a replacement of coarse NA with CSA is designated in this work as concrete with copper slag aggregate (CSAC). Within our own investigation, CSAC with two replacement ratios of NA was tested: CSAC\_20\_50 concrete in which 20% of 8/16 mm fraction and 50% of 16/31.5 mm fraction were replaced by volume with corresponding fractions of CSA, and CSAC\_50\_50 concrete in which 50% of 8/16 mm fraction and 50% of 16/31.5 mm fraction were replaced by volume with corresponding fractions of CSA. A control mix of concrete with only NA (NAC) was also tested. Standard methods used for the mix design and testing of NAC concrete can also be used for the design and testing of CSAC mixtures. Mix proportions of concrete together with tested compressive strength at 28 days and flow table results are presented in Table 1 [9]. The control concrete mixture was designed to meet the requirements for the C25/30 strength class.

The densities of fresh concrete mixtures CSAC\_20\_50 and CSAC\_50\_50 were higher by 4% and 5%, respectively, compared to the NAC. The density of hardened concrete mixtures CSAC\_20\_50 and CSAC\_50\_50 was higher by 5% and 7%, respectively, compared to the control mixture. This was due to the higher density of CSA grains compared to the NA grains. As shown in Table 1, mixtures CSAC\_20\_50 and CSAC\_50\_50 showed slightly larger compressive strengths at 28 days compared to NAC, the increase being equal to 12.4% and 10.5%, respectively. The cause of this increase was the higher compressive strength of CSA grains and better interaction between grains, due to their roughness and sharp edges.

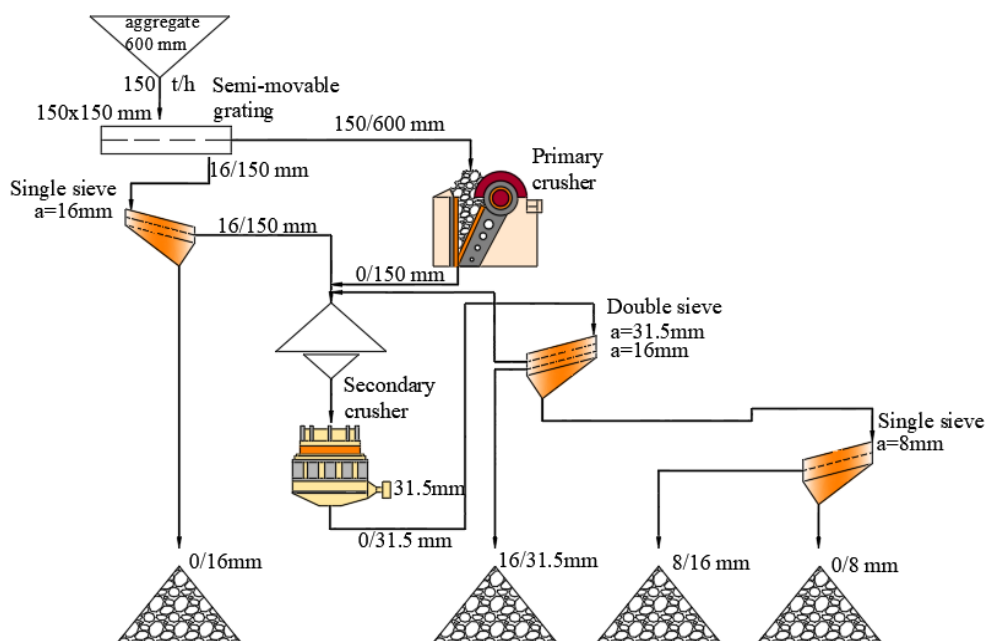


Figure 1. Copper slag plant technology

Table 1. Mix proportions, flow and compressive strength of tested NAC and CSAC [9]

Type of concrete	Cement (kg/m <sup>3</sup> )	Water (kg/m <sup>3</sup> )	Aggregate			w/c /	Flow (cm)	Compress. strength 28 days (MPa)
			Fine NA (river) (kg/m <sup>3</sup> )	Coarse NA (river) (kg/m <sup>3</sup> )	CSA (kg/m <sup>3</sup> )			
			NAC	398	212			
CSAC_20_50	398	212	732	753	394	0.533	32.0	40.8
CSAC_50_50	398	212	732	659	529	0.533	28.5	40.1

However, the replacement of NA with CSA caused the stiffer consistency of CSAC mixtures compared to the control mixture, as shown in Table 1. This occurred because the CSA grains had a larger specific surface area and less mobility. CSA grains are rougher and have sharper edges than NA grains, which causes greater friction between grains.

The water penetration resistance of the mixtures CSAC\_20\_50 and CSAC\_50\_50 was lower by 55.4% and 27.7%, respectively, compared to the NAC. At first sight, the result obtained in this way did not seem logical since the CSA itself had lower water absorption than NA. However, the water penetration resistance of concrete depends on the compactness of the concrete mixture, i.e., the presence of capillary pores in the cement stone. The increase in the volume of capillary pores in the concrete mixtures directly causes the decrease in the mixtures' water resistance. Although the same w/c ratio was used in all mixtures, due to the lower water absorption of CSA grains, the content of free water in the mixtures CSAC\_20\_50 and CSAC\_50\_50 was increased. The volume of capillary holes in concrete mixtures increased in direct proportion to the rise in free water.

Also, the increase in chloride penetration classified by the D<sub>RCM</sub> chloride migration coefficient was observed in the CSAC\_20\_50 mixture. The recorded effective chloride migration coefficient DRCM for the NAC showed a value of 39.7 x 10<sup>-12</sup> cm<sup>2</sup>/m, while for the CSAC\_20\_50 and CSAC\_50\_50 mixtures, DRCM was 46.8 x 10<sup>-12</sup> cm<sup>2</sup>/m and 36.0 x 10<sup>-12</sup> cm<sup>2</sup>/m, respectively. With a DRCM value higher than 16 x 10<sup>-12</sup>, all three mixtures could be suitable for use in environments without aggressive influences [20, 21]. However, as with water penetration resistance, the main

pattern of enhanced chloride migration through concrete is due to the increasing porosity of cement stone.

### 3 Environmental assessment

Environmental assessment was conducted using a well-recognized and standardized methodology for evaluating the environmental loads of processes and products during their life cycle - Life Cycle Assessment (LCA). According to ISO 14040 standards [22], LCA consists of four steps: (1) goal and scope definition, (2) creating the life cycle inventory (LCI), (3) assessing the environmental impacts (LCIA) and (4) interpreting the results.

#### 3.1 Goal, system boundaries, and functional unit (FU)

The goal of this study is to assess the environmental potential of replacing the NA with the CSA in the production of ready-mixed concrete. In the basic scenario, natural river aggregate was chosen instead of crushed aggregate since it is commonly used in Serbia. Within the CSAC mix design, two different replacement percentages of NA with CSA were tested: CSAC\_20\_50 and CSAC\_50\_50. Table 1 shows the mix proportions of the alternatives with the evaluated compressive strength after 28 days and the flow table results.

Having in mind this goal, a cradle-to-gate analysis was conducted, Figure 2, and the functional unit of 1 m<sup>3</sup> of ready-mixed NAC and CSAC was used in this work. The production of water was excluded from the analysis.

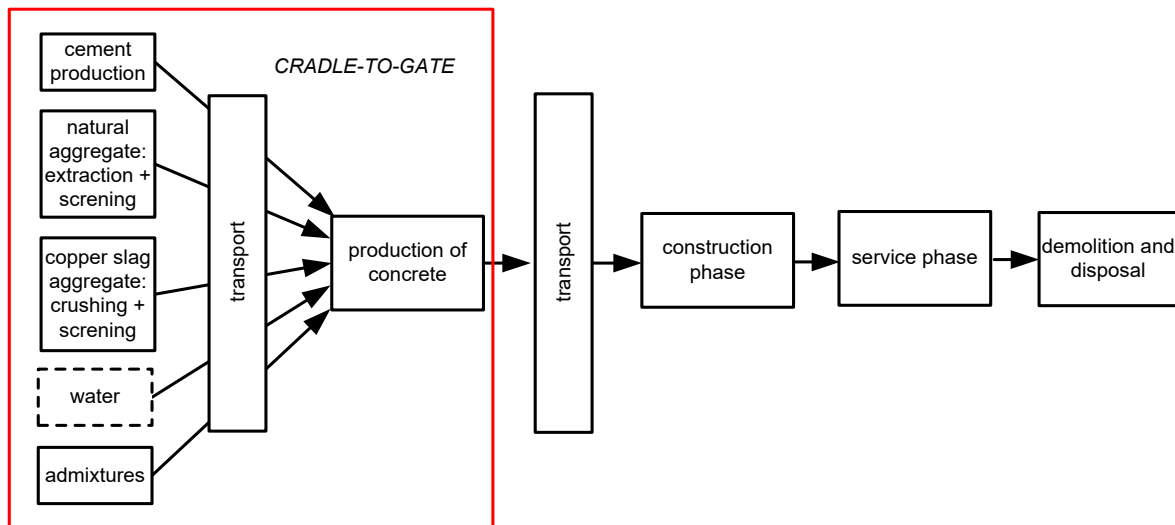


Figure 2. Cradle-to-gate part of the CSAC life cycle

3.2 Life cycle inventory (LCI) and transportation data

The production of ready-mixed NAC and CSAC studied in this paper is located in Bor, Serbia. All the LCI data for natural river aggregate, cement and concrete production was collected from local suppliers and manufacturers [23]. As for the CSA, data was collected from the flotation plant of the Mining and Smelting Basin Bor, where the copper slag is deposited at the landfill near the processing facilities. Since only naturally granulated copper slag was used in this research, the process for obtaining the copper slag consisted of sieving according to Figure 3. The electricity consumption is 0.28 kWh (1.01 MJ), while for the internal services, 0.704 l of diesel (24.8 MJ) is used per tone of aggregate. Emission data for diesel production and distribution, as well as for transportation that could not be collected for local conditions, was taken from the Ecoinvent V2.0 database [24, 25].

According to European Directive 2008/98/EC [26] any product that can bring revenue should not be considered as merely waste but as a useful by-product. This means that it carries a part of the environmental load of the primary process (copper production - main product), besides the load from its own treatment prior to utilization in concrete (secondary process – by-product). In the case of the application of various by-products or wastes as mineral additions or cement replacements in concrete, economic allocation is usually recommended over mass allocation. Because of the relatively large mass of by-products or wastes generated in primary processes, mass allocation has a significantly greater impact than economic allocation. This can certainly discourage producers for implementing such materials in making green concrete. However, since there is no market for CSA in Serbia, it was impossible to perform economic allocation between primary and secondary processes and copper slag was treated as waste in this work. In the basic scenario, the following transport distances were assumed. The concrete is produced in the concrete plant 'Metalka' in Bor, which is located 5 km away from a copper slag plant. Cement is transported by heavy trucks (16-32 t) from the cement factory 'CRH' – Popovac and the estimated distance is 50 km, while river aggregate is transported by medium-sized ships from 'Nova Separacija' – Paracin at an estimated distance of 50 km. Transport distances for each constituent material were doubled to account for the return trip.

3.3 Life cycle impact assessment - LCIA

Impact category indicators related to green-house gases and gases from burning fossil fuels were chosen in this study: global warming potential (GWP), eutrophication potential (EP), acidification potential (AP), and photochemical oxidant creation potential (POCP). They were calculated using the midpoint CML (the Institute of Environmental Sciences of the Faculty of Sciences of Leiden University) baseline methodology [27]. Besides, cumulated energy consumption within the studied part of the life cycle was calculated and expressed as energy use (EU). The LCI and LCIA calculations for each selected mixture were performed using original Excel-based software.

3.4 Sensitivity analysis

A sensitivity analysis was conducted to estimate the impact of the type of used NA and transport distance of CSA. Impacts were calculated for the case where NA was crushed stone instead of river aggregate, assuming the same mix design of concrete. Also, transport distances for CSA were varied from 5 km (as in the basic scenario) to 50 km, which is the assumed transport distance of other concrete constituent materials. Finally, impacts were calculated for the full technological scheme of processing (Figure 1), in which case the electricity consumption is 2.16 kWh (7.78 MJ), while for the internal services, 0.704 l of diesel (24.8 MJ) is used per tone of aggregate. Results are presented in chapter 4.

4 Results and discussion

The impact category indicators calculated for the basic scenario are presented in Figure 4.

The differences between the impacts of NAC and CSAC with both replacement ratios are within a few percent, they are practically equal. This is not surprising since the cement content in all alternatives is the same and cement is by far the largest contributor to all impacts. However, 394 kg/m<sup>3</sup> and 529 kg/m<sup>3</sup> of NA are preserved in the cases of CSAC<sub>20\_50</sub> and CSAC<sub>50\_50</sub>, respectively. In those cases, the generated waste is reduced by the same amount.

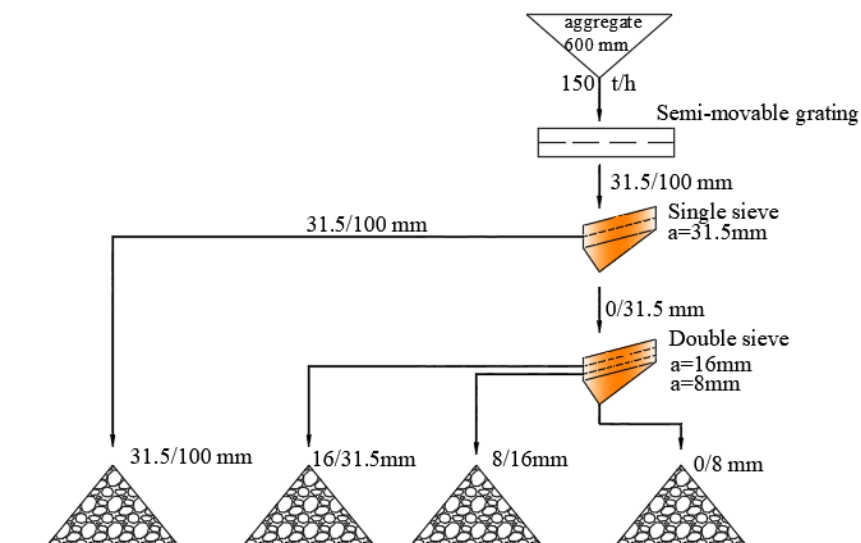


Figure 3. Sieving of copper slag at Mining and Smelting Basin Bor – basic scenario

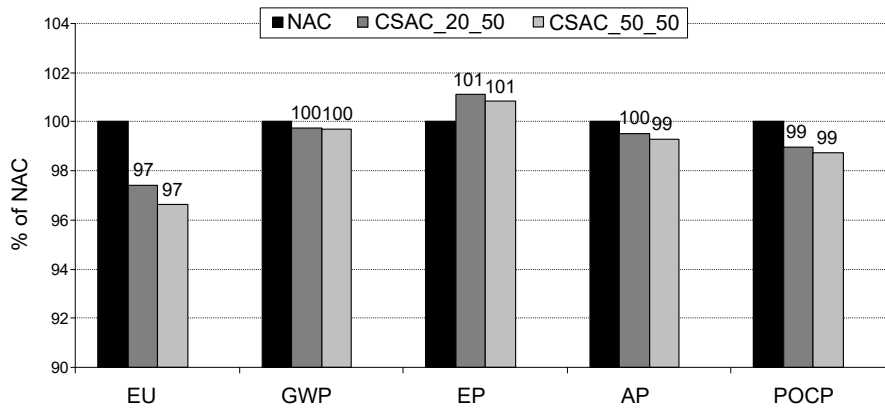


Figure 4. Impact category indicators per FU – basic scenario

If crushed NA is used instead of a river aggregate, the benefit of CSAC in energy use is greater, while other impact categories are similar, Figure 5. This is mostly the consequence of changed transportation type – crushed aggregates are transported by trucks instead of barges as was the case with river aggregate – which affects the NAC impacts more than CSAC impacts.

If the transportation distance of CSA in the basic scenario is changed from 5 km to 50 km, the calculated impact categories are shown in Figure 6. Energy use is now larger in the CSAC case, with all other impacts slightly larger. For all impacts to remain practically equal to the NAC impacts, the transportation distance of CSA should not be greater

than 20 km. Therefore, environmental benefits with CSAC through NA preservation and waste reduction can be obtained if the concrete is produced close to the CSA plant, within a distance of 20 km.

Finally, if the full technological processing scheme (Figure 1) for CSA production is applied, impacts are shown in Figure 7.

Impacts are very similar to those obtained in the basic scenario since the only difference is the larger energy use in the CSA production phase. However, this phase contribution is very small and cannot change total impacts by more than a few percent.

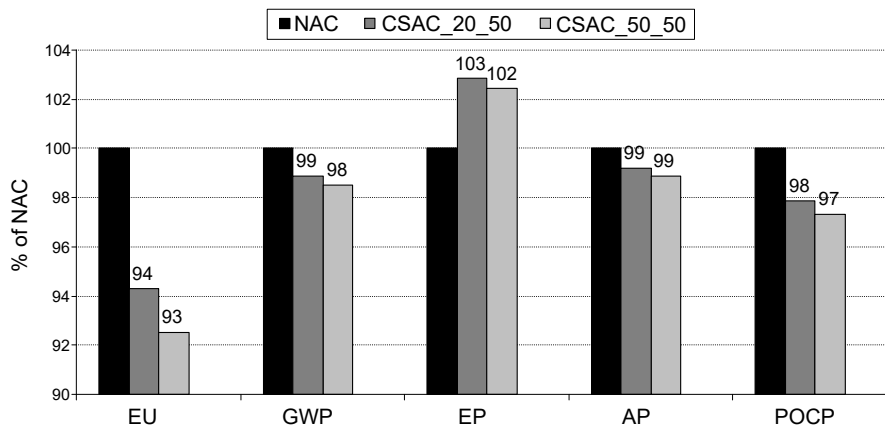


Figure 5. Impact category indicators per FU – crushed NA

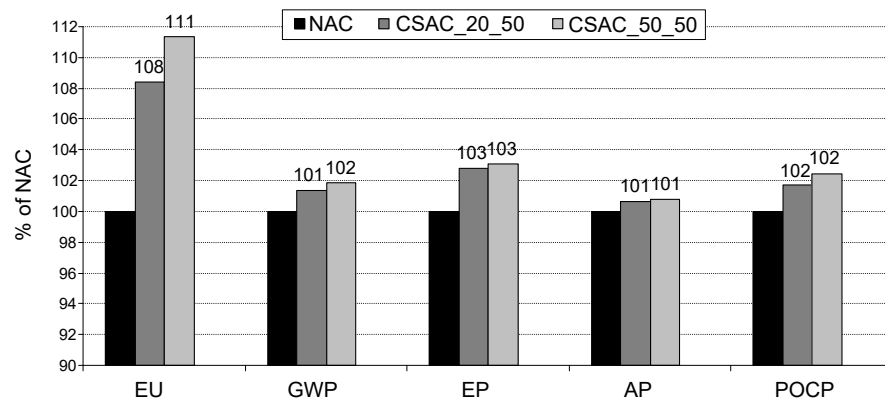


Figure 6. Impact category indicators per FU – all transport distances equal to 50 km

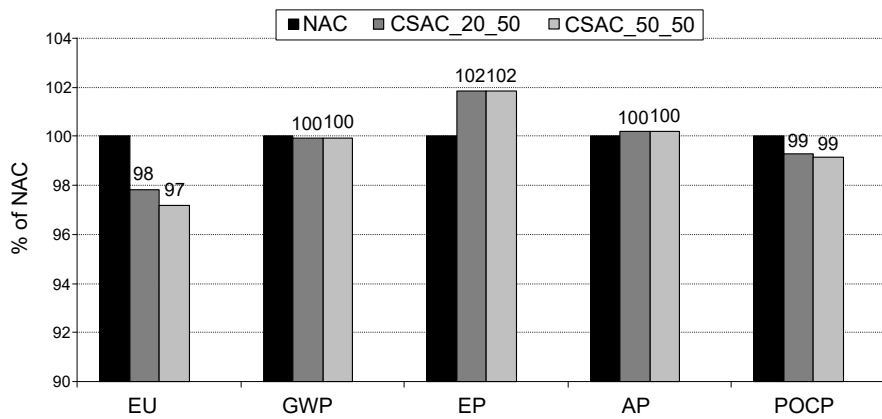


Figure 7. Impact category indicators per FU –full processing scheme

## 5 Conclusion

In this paper, the environmental potential of replacing the NA with aggregates produced from waste copper slag in concrete mix design was investigated. The conducted case study was based on Serbian LCI data and local conditions in the vicinity of the town of Bor in Serbia. Within these limits, and for chosen impact categories, it was concluded that CSA application in concrete can bring environmental benefits over NA application, in the form of NA preservation and waste reduction. This, however, is valid if the transport distances of CSA are lower than 20 km, so tested concrete mixtures are recommended for local applications.

The amount of waste materials used for the production of CSAC\_50\_50 makes up about 20% of the concrete unit weight. Yet this concrete can be used in structural applications where low-to-middle strength concrete is economically justified (for instance, in residential buildings). Having this in mind, it can be concluded that local applications of CSAC contribute to the preservation of natural bulk resources and landfill capacity, both becoming an important and scarce resource nowadays in many countries.

## Acknowledgment

This work was supported by the Ministry for Education, Science and Technological Development of the Republic of Serbia, research project Grant No. 451-03-9/2021-14/200052 and No. 200092, Faculty of Civil Engineering University of Belgrade. This support is gratefully acknowledged.

## References

- [1] C. Meyer, The Greening of the Concrete Industry, *Cement and Concrete Composites* 31 (2009) 601–605.
- [2] Q. Zhao, X. Liu, J. Jiang, Effect of Curing Temperature on Creep Behavior of Fly Ash Concrete, *Construction and Building Materials* 96 (2015) 326–333.
- [3] K.S. Al-Jabri, M. Hisada, A.H. Al-Saidy, S.K. Al-Oraimi, Performance of High Strength Concrete Made with Copper Slag as a Fine Aggregate, *Construction and Building Materials* 23 (2009) 2132–2140.
- [4] J. de Leeuw, D. Shankman, G. Wu, W.F.de Boer, J. Burnham, Q. He, H. Yesou, J. Xiao, Strategic Assessment of the Magnitude and Impacts of Sand Mining in Poyang Lake, China, *Regional Environmental Change* 10 (2010) 95–102.
- [5] G. Kuntikana, D.N. Singh, Contemporary Issues Related to Utilization of Industrial Byproducts, *Advances in Civil Engineering Materials* 6 (2017) 20160050.
- [6] P.S. Prasad, G.V. Ramana, Feasibility Study of Copper Slag as a Structural Fill in Reinforced Soil Structures, *Geotextiles and Geomembranes* 44 (2016) 623–640.
- [7] A. Maharishi, S.P. Singh, L.K. Gupta, Shehnazdeep, Strength and Durability Studies on Slag Cement Concrete Made with Copper Slag as Fine Aggregates, *Materials Today: Proceedings* 38 (2021) 2639–2648.
- [8] D. Urosevic, Copper Extraction from Smelting Slag by Combined Methods, The University of Belgrade, Technical Faculty in Bor, 2016.
- [9] S. Filipović, O. Đokić, A. Radević, D. Zakić, Copper Slag of Pyroxene Composition as a Partial Replacement of Natural Aggregate for Concrete Production, *Minerals* 11(2021) 439.
- [10] B. Gorai, R.K. Jana, Premchand, Characteristics and Utilisation of Copper Slag—a Review. *Resources, Conservation and Recycling* 39 (2003) 299–313.
- [11] C. Shi, C. Meyer, A. Behnood, Utilization of Copper Slag in Cement and Concrete. *Resources, Conservation and Recycling* 52 (2008) 1115–1120.
- [12] R. Neves, F. Branco, J. de Brito, Field Assessment of the Relationship between Natural and Accelerated Concrete Carbonation Resistance, *Cement and Concrete Composites* 41 (2013) 9–15.
- [13] M. Najimi, J. Sobhani, A.R. Pourkhorshidi, Durability of Copper Slag Contained Concrete Exposed to Sulfate Attack. *Construction and Building Materials* 25 (2011) 1895–1905.
- [14] K.S. Al-Jabri, R.A. Taha, A. Al-Hashmi, A.S. Al-Harthy, Effect of Copper Slag and Cement By-Pass Dust Addition on Mechanical Properties of Concrete, *Construction and Building Materials* 20 (2006) 322–331.
- [15] A. Dey, D. Dev, P. Saha, Use of Copper Slag as Sustainable Aggregate, *International Conference on Sustainable Civil Infrastructure* 1 (2014) 229–240.

- [16] K.S. Al-Jabri, M. Hisada, S.K. Al-Oraimi, A.H. Al-Saidy, Copper Slag as Sand Replacement for High Performance Concrete, Cement and Concrete Composites 31 (2009) 483–488.
- [17] A. Rajasekar, K. Arunachalam, M.Kottaisamy, Assessment of Strength and Durability Characteristics of Copper Slag Incorporated Ultra High Strength Concrete, Journal of Cleaner Production 208 (2019) 402–414.
- [18] A. R. Lori, A. Hassani, R. Sedghi, Investigating the mechanical and hydraulic characteristics of pervious concrete containing copper slag as coarse aggregate, Construction and Building Materials, 197 (2019) 130–142.
- [19] Achudhan, Deepavarsa, Vandhana, Khalida, Effect of Copper slag in Structural behaviour of Reinforced Concrete Beams, Materials Today: Proceedings, 5 (2018) 6878–6887.
- [22] I. Ugur, S. Demirdag, H. Yavuz, Effect of Rock Properties on the Los Angeles Abrasion and Impact Test Characteristics of the Aggregates, Materials Characterization 61 (2010) 90–96.
- [21] Q. Yuan, M. Santhanam, Erratum to: Test Methods for Chloride Transport in Concrete, (2013) E1–E1.
- [22] ISO, Environmental Management – Life Cycle Assessment, Set of International standards: ISO 14040-14043, Geneva, International Organization for Standardization, 2006.
- [23] S. Marinkovic, V. Radonjanin, M. Malesev, I. Lukic, Life Cycle Environmental Impact Assessment of Concrete, in L. Bragança, H. Koukkari, R. Blok, H. Gervasio, M. Veljkovic, Z. Plewako, R. Landolfo, V. Ungureanu, L.S. Silva, P. Haller (eds.), Sustainability of Constructions – Integrated Approach to Life-time Structural Engineering. COST action C25. Proceedings of Seminar: Dresden, 6-7 October 2008. Possendorf, Herstellung, Addprint AG, 3.5-3.16.
- [24] M. Spielmann, C. Bauer, R. Dones, M. Tuchschnid, Transport Services. Ecoinvent report no. 14., Swiss Cent. Life Cycle Invent., 2007.
- [25] R. Dones, C. Bauer, R. Bolliger, B. Burger, T. Heck, A. Röder, Paul Scherrer Institut, M.F. Emmenegger, R. Frischknecht, N. Jungbluth, M. Tuchschnid, ESU-services Ltd., Life cycle inventories of energy systems: results for current systems in Switzerland and other UCTE countries, Ecoinvent report. Dübendorf, 2007.
- [26] European Union, Directive 2008/98/EC of the European parliament and of the council on waste and repealing certain directives. Off J Eur Union L312, 2008, 3-30.
- [27] J.B. Guinée, M. Gorrée, R. Heijungs, G. Huppes, R. Kleijn, A. de Koning, L. van Oers, A. Wegener Sleswijk, S. Suh, H.A. Udo de Haes, H. de Bruijn, R. van Duin, M.A.J. Huijbregts, 2002. Handbook on life cycle assessment. Operational guide to the ISO standards. I: LCA in perspective. IIa: Guide. IIb: Operational annex. III: Scientific background. Kluwer Academic Publishers, Dordrecht, 2002.





## Durability performance of a lime stabilized expansive soil with egg shell ash as a subsidiary admixture

Sivapriya Vijayasimhan<sup>\*1)</sup>, Jijo James<sup>1)</sup>, Yuvaraj Karunanithi<sup>2)</sup>, Sushritha Gunipati<sup>2)</sup><sup>1)</sup> Associate Professor, Department of Civil Engineering, Sri Sivasubramaniaya Nadar College of Engineering, Kalavakkam, Chennai, India – 603110<sup>2)</sup> Undergraduate Students, Department of Civil Engineering, Sri Sivasubramaniaya Nadar College of Engineering, Kalavakkam, Chennai, India – 603110

### Article history

Received: 06 April 2022

Received in revised form:

02 June 2022

Accepted: 05 June 2022

Available online: 30 June 2022

### Keywords

stabilization;  
lime;  
egg shell ash;  
durability;  
sea water;  
compressive strength

### ABSTRACT

Stabilization is broadly classified as mechanical and chemical stabilization. Lime stabilization is the most commonly adopted method for stabilising expansive soils. In recent years, lime has been combined with other waste materials for improved performance in stabilization. One such waste is egg shell waste, generated by the poultry industry. Calcination of egg shell waste results in the formation of egg shell ash (ESA) which has a chemical composition very similar to that of quick lime. This investigation focuses on the potential of ESA as an auxiliary additive for lime in the stabilization of expansive soils. The initial consumption of lime of the expansive soil was determined using the Eades and Grim pH test. The lime content in the stabilization process was modified with ESA up to 0.5% in increments of 0.1%. Unconfined compression strength test samples of dimensions 38 mm x 76 mm were cast and cured for a period of 21 days and tested for their strength. The durability of the samples was also evaluated by subjecting the samples to 1, 4, 7, and 10 cycles of wetting and drying. The results of the investigation revealed that 0.2% ESA was the optimal dosage of additive to lime stabilization for improved performance.

## 1 Introduction

High plastic clays are problematic soils that are difficult to work with. They tend to exhibit a good amount of compressibility as well as a swelling nature due to variations in moisture content and applied loading conditions. Stabilization of such soils using chemical admixtures has been found to be effective, especially with the addition of lime. The addition of lime to such soils makes them friable and results in reduced plasticity and improved workability. However, recently, increasing investigations have focused on the effectiveness of lime stabilized soil under conditions of durability like wetting-drying, freeze-thaw, and extreme variations in pH, to name a few. These investigations have brought out the lack of effectiveness of lime stabilized soil under such conditions. Several researchers have attempted to augment the performance of lime stabilization by substitution as well as auxiliary addition of solid wastes [1]. Utilization of wastes is based on the possibility of augmenting the potential of lime by either increasing the supply of calcium ions or providing silica and alumina to enhance the pozzolanic reactions. There are several waste materials that have been adopted in soil stabilization for their effective reuse while also achieving beneficial results in soil improvement [2]. One such waste material that is generated in significant quantities in India is eggshell waste (ESW).

India produced as many as 103.32 billion eggs in the year 2018-2019 [3]. Taking 5.5 grams as the average shell weight of an egg [4], the estimated ESW generated in India is as high as 568,260 tonnes. This quantity of waste is definitely a strain on the solid waste management system. Utilization of these wastes in Civil Engineering applications, including concrete, bricks and blocks, and soil stabilization, is therefore desirable. Egg shell waste is basically rich in calcium carbonate. Carbonate lime is not very reactive and is mostly inert [5]. Hence, it is not preferred for stabilization of soil. However, ESW can be activated into a more reactive form by calcining it at a sufficiently high temperature, which converts it into eggshell ash (ESA). ESA is very similar in composition to quick lime [6]. There are quite a few investigations involving the use of ESW. However, the use of ESA in Civil Engineering applications has started to gain traction recently. Its use in soil stabilization is still evolving and has a lot of potential for achieving beneficial modifications in soil engineering. Okonkwo et al. [6] investigated the potential of utilizing ESA in combination with cement in stabilizing lateritic soil. They found that 8% cement with 10% ESA resulted in the maximum strength of the lateritic soil.

\* Corresponding author:

E-mail address: [sivapriyavijay@gmail.com](mailto:sivapriyavijay@gmail.com)

James and Pandian [7] attempted to study the effect of ESA on the development of the early strength of a lime stabilized soil. Their investigation revealed that the addition of 0.5% ESA was capable of enhancing the early strength of 5.5% lime stabilized soil by 10% at 7 days of curing. James et al. [4] investigated the possibility of ESA being utilized in lime stabilization of an expansive soil as an auxiliary additive. Their investigation revealed that addition of 2% ESA along with 4% lime was able to generate a 24.43% increase in the strength of the expansive soil at 28 days of curing and reduce its plasticity by almost 7%. Bensaifi et al. [8] delved into the influence of crushed granulated blast furnace slag and calcined eggshell waste on the mechanical properties of compacted marl. They found that a 15% dosage of a combination of the slag and calcined egg shell waste was capable of developing the maximum strength and bearing. Ayodele et al. [9] evaluated the performance of combinations of sawdust ash and ESA in the stabilization of lateritic blocks. They concluded that the combination of sawdust ash and ESA can be used as a viable alternative to cement in the stabilization of blocks. Yie [10] researched the stabilization of soft clay using combinations of silica fume and ESA. His investigation revealed that 6% silica fume with 6% ESA was able to increase the unconfined compression strength by 69%.

Afolayan et al. [11] looked into the prospects of using ESA as a replacement for cement in the manufacture of sandcrete blocks. They found that ESA could replace up to 30% of cement without much loss in the strength of the block. James et al. [12], in a later investigation, attempted to study the potential of ESA as a potential replacement for lime in the stabilization of lime under conditions of wetting and drying (WD). They found that increasing ESA in the mix resulted in more durability of the stabilized soil. Looking at the available literature, it is clear that ESA is a waste material with good potential for soil stabilization. However, the focus of the majority of the investigations was only on the strength of the stabilized soil or blocks. However, there is a need to study the durability of ESA stabilized soil under varying conditions. This investigation focuses on the durability of lime stabilized soil modified with ESA when it is subjected to alternate cycles of WD in faucet (tap) water as well as seawater.

## **2 Materials and methodology**

The various materials used in this investigation were the virgin soil, hydrated lime for its stabilization, ESA (used as the subsidiary admixture), tap water, and sea water as the weathering agents for durability study.

### **2.1 Materials**

The soil used in conducting the experiments was collected from the banks of the Thaiyur Lake, Kalavakkam near Chennai, India. The soil sample has a large percentage of clay content with 68.7%, silt at 28.4%, and 2.9% of sand. The collected soil is oven dried for characterisation using the relevant Indian standard code; it has a specific gravity of 2.76, a liquid limit of 75.8%, a plastic limit of 23.5% and a shrinkage limit of 11.2%. From the obtained results, the soil is classified as high compressible clay (CH).

High quality industrial grade calcium hydroxide, also called as hydrated lime, procured from M/s. Shiyal Chemicals, India, was used in the experiments.

ESA was obtained by calcining egg shells in a muffle furnace. The egg shell waste for manufacture of ESA was obtained from SKM Egg Products, Erode. The obtained egg shell waste was in crushed form, free from proteins and organic content. It was further pulverized and sieved to obtain a fine powder of particle size finer than 75 microns. This powder was calcined in a muffle furnace at a temperature of 500°C for a period of 15 minutes to obtain ESA.

### **2.2 Experimental methodology**

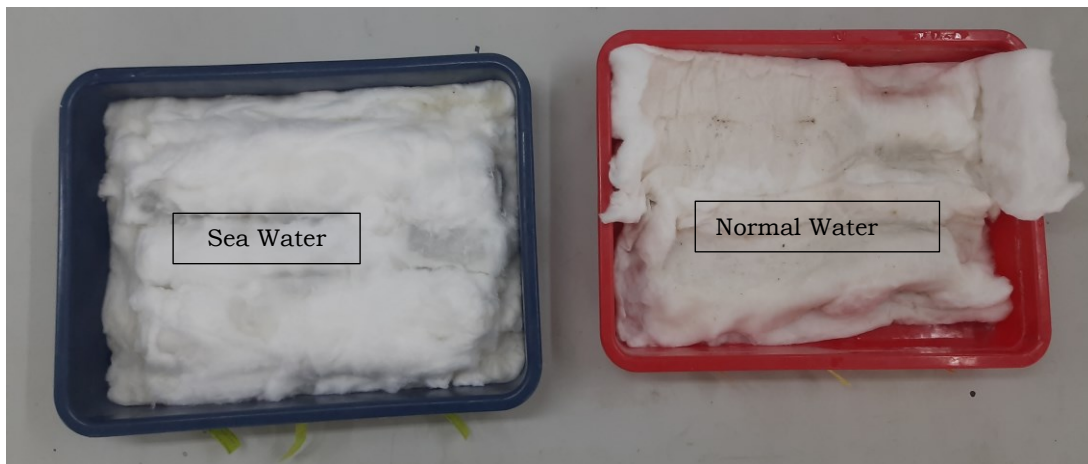
The experimental programme began with the characterization of the soil collected. It was subjected to various geotechnical properties tests, including liquid limit and plastic limit [13], shrinkage limit [14], specific gravity [15], grain size distribution [16], compaction characteristics [17], unconfined compression strength (UCS) [18], and classified based on the BIS code [19]. The soil was then subjected to the Eades and Grim pH test [20] in accordance with ASTM code [21] for the determination of Initial Consumption of Lime (ICL). After the determination of ICL, the compaction characteristics of the soil-lime mix were determined using the mini compaction test method proposed by Sridharan and Sivapullaiah [22], in accordance with the BIS code for stabilized soils [23]. After the determination of compaction characteristics, particles passing 2 mm sieve were used to find the UCS of the soil with a 38 mm diameter and 76 mm height cylindrical split mould, compacted to its maximum dry unit weight at its optimum moisture content. With the known dry unit weight, the quantity of the sample for the test was back calculated. The soil, lime and ESA were initially hand mixed in dry conditions for a minimum duration of 10 minutes until a homogeneous mix was obtained, before adding water. Following this, the computed quantity of water based on the compaction characteristics was sprinkled and a uniform mix was prepared. To maintain uniform preparation of samples, the same duration of mixing was followed for all the combinations. This was then packed into the split mould and compacted using static compaction. The results were obtained from the average of three samples after a curing period of 21 days in sealed polythene covers for various combinations. The quantity of ESA was increased in increments of 0.1% up to 0.5% by weight of dry soil to determine the optimum dosage of ESA for maximum strength. The mix proportions of soil, lime, and ESA are shown in Table 1. To understand the durability behaviour of the soil with admixtures, samples were prepared for the optimum percentage of ESA and cured with faucet, i.e., tap and sea water. The durability of the specimens was determined by wrapping the samples in a bed of cotton and placing them in a tray which was drenched with normal tap and sea water for a period of 24 hours. This was followed by a period of 24 hours wherein the samples were placed in the open air at room temperature. This constituted one cycle of WD. Samples were subjected to 1, 4, 7, and 10 cycles of WD (figure 1) after 21 days of air curing. The tap water used had a pH value of 6.9 while the sea water, collected from Thiruvannamiyur beach, Tamil Nadu, India, had a pH value of 7.9.

Table 1. Mix Proportions

Mix Proportion	Notation	Soil (%)	Lime (%)	ESA (%)
Soil + 4.5%L	SLE0	95.69	4.31	0.00
Soil + 4.5%L + 0.1%ESA	SLE1	95.60	4.30	0.10
Soil + 4.5%L + 0.2%ESA	SLE2	95.52	4.29	0.19
Soil + 4.5%L + 0.3%ESA	SLE3	95.42	4.29	0.29
Soil + 4.5%L + 0.4%ESA	SLE4	95.33	4.29	0.38
Soil + 4.5%L + 0.5%ESA	SLE5	95.24	4.29	0.47



a. Prepared sample



b. Sample under WD process

Figure 1: Sample for testing

### 3 Results and discussion

The maximum dry unit weight of the virgin soil was 13.34 kN/m<sup>3</sup> with an optimum moisture content of 28.2%. The ICL of the soil found using the Eades and Grim method was 4.5%. The maximum unit weight value of modified clay with ICL was 12.74 kN/m<sup>3</sup> and the optimum moisture content was 32.23%. The samples were prepared at their optimum levels to obtain their strength properties.

#### 3.1 UCS of lime stabilized soil modified with ESA

Figure 2 shows the performance of ESA amended lime stabilized soil. It is seen that the addition of ESA to the mix results in an overall increase in the strength of the stabilized soil, irrespective of the content of ESA. All dosages generated strength higher than the strength of the virgin soil as well as lime stabilized soil. Similar increases in strength due to the addition of ESA to lime in the stabilization of soil have also been reported by other researchers [4], [7]. It is

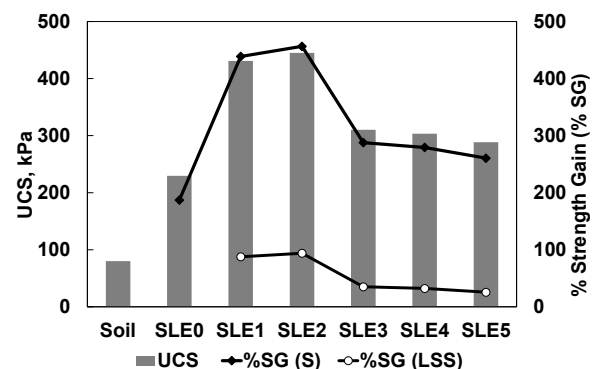


Figure 2. Performance of ESA amended lime stabilized soil

also obvious that an ESA content of 0.2% is the optimum dosage for the development of maximum strength. The strength of the virgin soil increased from 80 kPa to 229.5 kPa for 4.5% lime stabilization at 21 days of curing. With the

addition of 0.2% dosage of ESA with 4.5% lime, the strength further increases to 445.1 kPa. Earlier, James and Pandian [7] reported an optimum ESA content of 0.5% and an ICL of 5.5% for the soil in their investigation. With a further increase in the ESA content of the stabilized soil, the strength of the soil is reduced. However, the strength was still higher than the strength of the virgin soil as well as the lime stabilized soil. Beyond an ESA content of 0.3%, the reduction in strength of the soil was less and more or less stable as seen from the height of the bars. Thus, it can be concluded that the addition of small quantities of ESA will definitely result in a beneficial effect on the strength of the lime stabilized soil.

Figure 2 also shows the percentage strength gain (%SG) due to the addition of lime and ESA to the mix. The line with solid markers represents the %SG of the stabilized soil, computed based on the strength of the virgin soil, denoted by %SG (S) in the figure. The addition of 4.5% lime results in a %SG of 187% compared to the strength of the virgin soil. It can also be seen that all doses of ESA produce a significant gain in the strength of the stabilized soil. The addition of 0.5% ESA results in a minimum strength gain of 260.5%. The addition of 0.1% and 0.2% ESA results in a strength gain of 438.7% and 456.5%, respectively, when compared to virgin soil. In order to understand the contribution of ESA to the strength development, the %SG was also computed based on the strength of the lime stabilized soil. The line with hollow markers represents the %SG of the stabilized soil computed based on the strength of 4.5% lime stabilized soil, denoted by %SG (LSS) in the figure. The addition of 0.1% ESA increases the strength of the lime stabilized soil by 87.7%, whereas 0.2% ESA increases it by 93.9%. A further increase in ESA content results in a drop in %SG to 25.6% when ESA content is increased to 0.5%. However, all doses of ESA considered in this investigation were capable of further augmenting the strength of the lime stabilized soil. Table 2 shows the strength results of all the combinations tested in this investigation.

It can also be seen from the strength gain figures that the dosages divide the stabilization into two zones at 0.2%. The strength values below 0.2% are comparable, whereas the strength values beyond 0.2% are comparable as well. Nasrizar et al. [24] identified the boundaries of ICL and optimum lime content (OLC), dividing lime stabilization into three phases. However, the boundary seen in the results may be limited only to the present investigation, and more future investigations are essential to identify the presence of such boundaries in ESA modified soil. Thus, ESA being very similar to lime in composition, there are possibilities of boundaries existing in the stabilization process which involves ESA.

Figure 3 shows a comparison between the present study and earlier studies involving ESA. In order to bring in the effect of both the stabilizers into the comparison, the composition of the stabilizers has been reduced to an ESA/Lime ratio as done in some earlier investigations [12], [25], [26]. Most of the work with egg shell waste predominantly deals with egg shell powder. To enhance the

effective usage of the egg shell waste, it is further calcined and used as a subsidiary material in the modified soil. Very few researchers have addressed this in their investigations, especially since the combination of lime and eggshell ash is virtually absent in literature. Two earlier studies done by James et al. in the year 2017 [4] and 2020 [12] were considered for comparison due to their similarities with the present study viz. use of combinations of lime and ESA in stabilization of a highly plastic soil. The authors of the present investigation were unable to find any other similar research using the combination of lime and ESA for comparison. Pure lime stabilization results have not been included in the comparison. Before the actual interpretation of the comparison, it is imperative to list out the limitations of the comparison. (i) The soil stabilized using the combinations of ESA and lime in each of these investigations is not the same and, hence, forms the first and foremost impediment in bringing the results to the same plane. (ii) The available data for the previous two studies were for 28-day cured samples, whereas in the present study they were for 21-day cured samples. (iii) The conditions of testing in laboratory-controlled conditions may not be the same for the three studies.

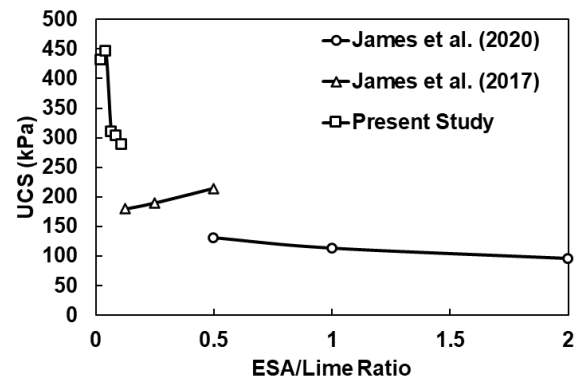


Figure 3. Comparison of present study with previous studies

The figure reveals the fact that the strength test results obtained in the present study are the highest of the three studies compared. A look at the comparison also reveals the fact that the strength values of the stabilized soil are higher when the ESA/lime ratio is lower. On the whole, when the ESA/lime ratio is lower than 0.5, the strength values are higher. This is somewhat in agreement with the conclusion given by James et al. [12], who recommended adopting ESA/lime ratios of less than one. Another important point to be noted is that in the work done by James et al. [12], ESA was used as a replacement for lime, as a result of which the minimum quantity of lime required for stabilization was not maintained. This may have been a reason for the low development of strength in their study. To summarize, lower ratios of ESA/lime can provide greater benefits when compared to higher ratios

Table 2. UCS (kPa) and % SG of all combinations

Parameter	Soil	SLE0	SLE1	SLE2	SLE3	SLE4	SLE5
UCS	79.98	229.54	430.87	445.08	310.14	303.34	288.34
%SG (S)	-	187	438.7	456.5	287.8	279.3	260.5
%SG (LSS)	-	-	87.7	93.9	35.1	32.1	25.6

### 3.2 Durability of ESA modified lime stabilized soil

The durability of the stabilized soil was determined by studying the strength of the stabilized specimens after they were subjected to 1, 4, 7, and 10 cycles of WD. The samples which were not subjected to any cycles were considered the control specimens. Figure 4 shows the effect of WD on the strength of the ESA modified lime stabilized soil. It is clear that the effect of WD results in a reduction in the strength of the stabilized soil. For the samples immersed in tap water, there is a drastic reduction in strength till 7 cycles of WD, whereas in the case of samples immersed in sea water, there is a significant reduction in strength of the specimens until 4 cycles of WD. The strength of the samples drops from 445.1 kPa to just 105.1 kPa after 7 cycles of WD. At 10 cycles of WD, the strength marginally increases to 110.85 kPa, which is still higher than the strength of pure lime stabilized soil under normal conditions.

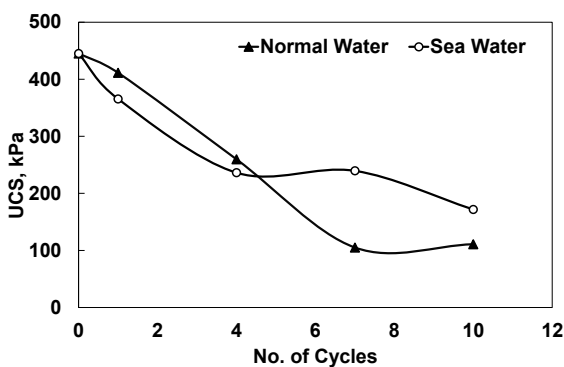


Figure 4. Durability of ESA modified lime stabilized soil subjected to WD

In the case of sea water weathering, the initial strength of the specimens is lower than that of the tap water weathering. However, after 4 cycles of WD, the specimens resist loss in strength much better than specimens subjected to tap water weathering. The strength of the samples reduces from 445.1 kPa to 236.2 kPa at 4 cycles of WD and thereafter drops to 171.8 kPa at 10 cycles of WD. This is significantly higher than the strength of pure lime stabilized soil. Kavak et al. [27] as well as Bilgen et al. [28] report that stabilized soil specimens prepared with sea water developed higher strength when compared to those with tap water. Kavak et al. [27] attributed this to the flocculation effect of salt present in seawater. As a result, the deterioration of the strength of the specimens in sea water is lower than in tap water. Table 3. shows the UCS of the optimally modified soil after different cycles of wetting and drying in normal and sea water.

To better understand the durability of the stabilized specimens in the present study, the strength index ( $I_{qu}$ ) of the stabilized soil specimens was determined. Muntohar and Khasanah [29] report the strength index to be the ratio of the strength of the stabilized specimen subjected to WD cycles to that of the strength of the specimens not exposed to WD. Figure 5 shows the strength indices of the ESA modified stabilized soil along with the results of the work done by

Table 3. UCS (kPa) of optimally modified soil after various cycles of wetting and drying

Agent / Cycles	0	1	4	7	10
Normal Water	445.08	411.32	259.68	105.08	110.85
Sea Water	445.08	365.50	236.21	239.50	171.79

James et al. [12]. They considered only up to 5 cycles of WD in their investigation. The total binder content was 3%, in which the lime/ESA ratio was varied as 2:1, 1:1, and 1:2. For the purpose of comparison, the data from the present study is limited to 7 cycles, as the other study investigated only up to 5 cycles. At the outset, it is clear that the strength index of the specimens tested in the present study steadily decreases. In the case of the samples subjected to seawater weathering, the strength index stabilizes after 4 cycles of WD. Comparing the results of the present study with those of James et al. [12], it can be seen that their strength indices are lower than those of the specimens in the present study, with the exception of LE12. The combination LE12 has an increase in strength index with increase in the number of WD cycles. This may be mainly due to the fact that the proportion of ESA was double that of lime in the mix. ESA is rich in calcium oxide, which is more reactive when compared to hydrated lime. The immersion of the specimen would have supplied additional water content required for hydration of this calcium oxide from ESA, resulting in an increase in strength. Thus, it was found that the durability of the ESA modified lime stabilized soil was much better in saline environments when compared to normal environments. However, more detailed investigations are required to understand the mechanism behind the improved resistance using microstructural studies.

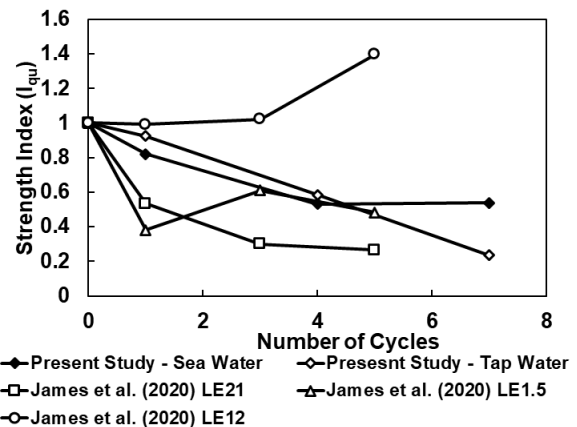


Figure 5: Strength index of stabilized specimens

### 3.3 Stress-strain characteristics of ESA modified lime stabilized soil

Figure 6 shows the stress-strain characteristics of the lime stabilized soil modified with an optimal dosage of ESA and subjected to cycles of WD. The sample not subjected to WD has been taken as the control specimen. For the sake of clarity, the samples subjected to 1, 4, and 10 cycles alone have been shown along with the control specimen. It is clear that 0.2% ESA modified lime stabilized soil exhibits brittle behaviour, with the failure strain at 1.07%. The first cycle of WD in normal tap water (T) results in an increase in the brittleness of the specimen with the failure strain reduced to 0.7%, However, the peak stress also reduces marginally.

But, on the other hand, WD in seawater (S) results in a slight reduction in brittleness with a lowered peak stress and increased failure strain at 1.45%. The first cycle of WD has different effects on the stabilized soil specimens due to the difference in the fluid to which the specimens were exposed. With an increase in the number of cycles of WD to 4 cycles, the behaviour of the specimens, both in tap water and seawater, exhibits an increased ductile behaviour with a significant reduction in peak stress and an increase in corresponding peak strain. The specimen in seawater had a peak failure strain of 2.37%, whereas the specimen in tap water had a peak strain of 2.89%, both of which are significantly higher than the failure strains in the first cycle. At this stage, both tap water as well as seawater cycled specimens exhibit more or less similar stress-strain characteristics. After 10 cycles of WD, specimens in both tap water as well as seawater seem to have recovered some of their brittle nature, though the peak stress is significantly reduced when compared to the control. The failure strains were 1.05% and 1.18% for seawater and tap water cycled specimens, respectively. At this stage, specimens in seawater seem to have developed more stiffness when compared to tap water cycled specimens. Based on the stress-strain characteristics, it can be inferred that WD cycles significantly influence the stress-strain characteristics of the specimens. Moreover, the type of pore fluid also significantly influences the stress-strain behaviour. Lastly, the extent of exposure to different pore fluids can result in different stress-strain behaviours, as seen from the opposing stiffness behaviours at the start and end of the durability cycles for tap water and seawater cycled specimens. However, the durability of specimens in seawater is not as frequently investigated as in normal tap water. More detailed investigations with various controls can reveal a much better picture of the stress-strain behaviour of such stabilized specimens.

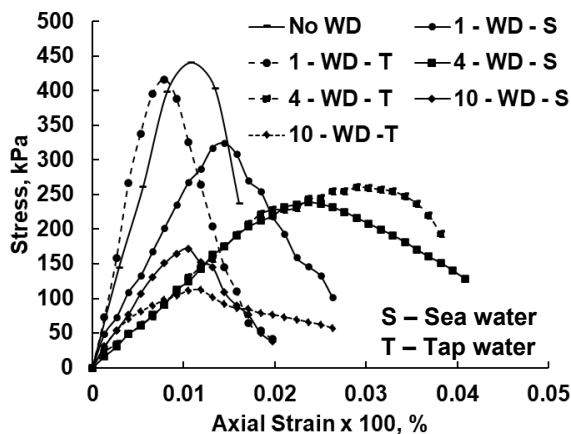


Figure 6: Stress - strain behaviour of ESA modified lime stabilized soil

#### 4 Conclusion

The use of sustainable material to increase the shear strength of the soil has been heavily researched by many researchers in recent times. With advancements in technology, poultry and agricultural by-products are also

used after processing or calcinating them to modify the properties of the soil by mixing them in various portions.

In this study, egg shell obtained from poultry is calcined and mixed with ICL content to modify the shear strength of a problematic soil. ESA was added to the soil in concentrations ranging from 0.1% to 0.5%, and experiments were carried out. To understand the durability characteristics of ESA + ICL in soil, the WD process was carried out with tap and sea water for 1, 4, 7, and 10 cycles. The following observations were made from the test results.

1. The ILC of the soil was found to be 4.5%; for this soil, the optimum percentage of ESA was 0.2%. With the addition of 4.5% lime to the soil, the shear strength increases from 79.98 kPa to 229.54 kPa, which is 2.87 times. The addition of 0.2% ESA to 4.5% lime stabilized soil results in the strength further increasing to 445.1 kPa, an increase of 1.93 times. Beyond the addition of 0.2% of ESA with lime to the soil, the role of ESA diminishes in increasing the strength of the soil, but the UCS value at 0.5% ESA is almost 1.26 times that of the pure lime stabilized soil. This indicates that the role of ESA in stabilization is appreciable.

2. The optimal dosage of 0.2% ESA seems to divide the stabilization into different stages. There is a possibility that such boundary values may exist for ESA just like ICL and optimum lime content (OLC) exist for lime stabilization, which needs to be further researched.

3. When the ratio of ESA/lime reduces, the UCS of the soil increases. This is true both for ESA as an additive as well as ESA as a replacement, as seen in a previous study. Thus, it can be concluded that lower ratios of ESA/lime are more beneficial in stabilization. Further research can be carried out to establish this for other types of soils and conditions.

4. The increase in the number of WD cycles with tap and sea water reduces the strength of the soil. With an increase in the number of cycles, the WD process with sea water shows better performance than with tap water, which is due to the speedy reaction of hydrated lime with the cations of ESA and sea water, making the soil flocculated. Thus, it can be stated that ESA modification of lime stabilization can be adopted in the stabilization of soils exposed to seawater.

5. Based on the stress-strain response, it can be stated that the stress-strain behaviour of the soil is influenced by WD conditions, the type of pore fluid, as well as the extent of exposure, resulting in varying behaviours. But, durability against exposure to seawater needs more research to better explain the behaviour of such stabilized soils in the aforementioned conditions.

This investigation reveals some interesting information that can be researched in future investigations. The existence of boundaries in stabilization stages for ESA can be researched (like ICL or OLC exists for lime). The effect of the ratio of ESA/lime when lime content is below ICL, between ICL and OLC, and above OLC can be further researched for a better understanding of optimizing ESA in lime stabilization. With decreasing sources of good quality water, the potential of seawater as a potential hydrating agent as well as a curing agent can be studied in future investigations.

#### Acknowledgment

The authors are grateful to SSN Trust, India for financial support.

## References

- [1] J. James and P. K. Pandian, "Industrial Wastes as Auxiliary Additives to Cement / Lime Stabilization of Soils," *Adv. Civ. Eng.*, vol. 2016, no. Article ID 1267391, pp. 1–17, 2016, doi: doi.org/10.1155/2016/1267391.
- [2] J. James and P. K. Pandian, "Soil Stabilization as an Avenue for Reuse of Solid Wastes : A Review," *Acta Tech. Napocensis Civ. Eng. Arch.*, vol. 58, no. 1, pp. 50–76, 2015.
- [3] BAHS, "Basic Animal Husbandry Statistics," 2019. [Online]. Available: [http://dahd.nic.in/sites/default/files/BAHS \(Basic Animal Husbandry Statistics-2019\)\\_0.pdf](http://dahd.nic.in/sites/default/files/BAHS%20(Basic%20Animal%20Husbandry%20Statistics-2019)_0.pdf)  
[http://dahd.nic.in/sites/default/files/BAHS \(Basic Animal Husbandry Statistics-2019\)\\_0.pdf](http://dahd.nic.in/sites/default/files/BAHS%20(Basic%20Animal%20Husbandry%20Statistics-2019)_0.pdf).
- [4] J. James, P. K. Pandian, and A. S. Switzer, "Egg Shell Ash as Auxiliary Addendum to Lime Stabilization of an Expansive Soil," *J. Solid Waste Technol. Manag.*, vol. 43, no. 1, pp. 15–25, 2017.
- [5] J. James and P. K. Pandian, "Performance Study on Soil Stabilisation using Natural Materials," *Int. J. Earth Sci. Eng.*, vol. 6, no. 1, pp. 194–203, 2013.
- [6] U. N. Okonkwo, I. C. Odiong, and E. E. Akpabio, "The Effects of Eggshell Ash on the Strength Properties of Cement Stabilized Lateritic," *Int. J. Sustain. Constr. Eng. Technol.*, vol. 3, no. 1, pp. 18–25, 2012.
- [7] J. James and P. K. Pandian, "Development of Early Strength of Lime Stabilized Expansive Soil: Effect of Red Mud and Egg Shell Ash," *Acta Tech. Corviniensis - Bull. Eng.*, vol. 9, no. 1, pp. 93–100, 2016.
- [8] E. Bensaifi, F. Bouteldja, M. S. Nouaouria, and P. Breul, "Influence of crushed granulated blast furnace slag and calcined eggshell waste on mechanical properties of a compacted marl," *Transp. Geotech.*, vol. 20, no. 100244, pp. 1–9, 2019, doi: 10.1016/j.trgeo.2019.100244.
- [9] A. L. Ayodele, O. M. Oketope, and O. S. Olatunde, "Effect of sawdust ash and eggshell ash on selected engineering properties of lateralized bricks for low cost housing," *Niger. J. Technol.*, vol. 38, no. 2, p. 278, 2019, doi: 10.4314/njt.v38i2.1.
- [10] L. S. Yie, "Undrained Shear Strength of Soft Clay Stabilised With Eggshell Ash and Silica Fume," Universiti Malaysia Pahang, 2019.
- [11] J. O. Afolayan, F. O. P. Oriola, G. Moses, and J. E. Sani, "Investigating the effect of eggshell ash on the properties of sandcrete block," *Int. J. Civ. Eng. Constr. Estate Manag.*, vol. 5, no. 3, pp. 43–54, 2017, [Online]. Available: <https://www.researchgate.net/publication/319493954>.
- [12] J. James, P. Jothi, P. Karthika, S. Kokila, and V. Vidyasagar, "Valorisation of egg shell ash as a potential replacement for lime in stabilization of expansive soils," *Gradjevinski Mater. i Konstr.*, vol. 63, no. 3, pp. 13–20, 2020, doi: 10.5937/grmk2003013j.
- [13] BIS, *IS 2720 Methods of Test for Soils:Part 5 Determination of Liquid and Plastic Limit*. India, 1985, pp. 1–16.
- [14] BIS, *IS 2720 Methods of Test for Soils:Part 6 Determination of Shrinkage Factors*. India, 1972, pp. 1–12.
- [15] BIS, *IS 2720 Methods of Test for Soils Part 3:Determination of Specific Gravity/Section 1 Fine Grained Soils*. India, 1980, pp. 1–8.
- [16] BIS, *IS 2720 Methods of Test for Soils:Part 4 Grain Size Analysis*. India, 1985, pp. 1–38.
- [17] BIS, *IS 2720 Methods of Test for Soils:Part 7 Determination of Water Content-Dry Density Relation Using Light Compaction*. India, 1980, pp. 1–9.
- [18] BIS, *IS 2720 Methods of Test for Soils:Part 10 - Determination of Unconfined Compressive Strength*. India, 1991, pp. 1–4.
- [19] BIS, *IS 1498 Classification and Identification of Soils for General Engineering Purposes*. India, 1970, pp. 4–24.
- [20] J. L. Eades and R. E. Grim, "A Quick Test to Determine Lime Requirements for Lime Stabilization," *Highw. Res. Rec.*, vol. 139, pp. 61–72, 1966.
- [21] ASTM, *D6276 Standard Test Method for Using pH to Estimate the Soil-Lime Proportion Requirement*, vol. 14. United States, 2019, pp. 1–4.
- [22] A. Sridharan and P. V. Sivapullaiah, "Mini compaction test apparatus for fine grained soils," *Geotech. Test. J.*, vol. 28, no. 3, pp. 240–246, 2005, doi: 10.1520/gtj12542.
- [23] BIS, *IS 4332 Methods of Test for Stabilized Soils:Part 3 Test for Determination of Moisture Density Relations for Stabilized Soil Mixtures*. India, 1967, pp. 1–12.
- [24] A. A. Nasrizar, K. Ilamparuthi, and M. Muttharam, "Quantitative Models for Strength of Lime Treated Expansive Soil," in *GeoCongress 2012, March 25-29, Mar.* 2012, pp. 978–987, doi: 10.1061/9780784412121.101.
- [25] J. James, P. K. Pandian, K. Deepika, J. M. Venkatesh, V. Manikandan, and P. Manikumar, "Cement Stabilized Soil Blocks Admixed with Sugarcane Bagasse Ash," *J. Eng.*, vol. 2016, no. Article ID 7940239, pp. 1–9, 2016, doi: doi.org/10.1155/2016/7940239.
- [26] J. James and R. Saraswathy, "Performance of Fly Ash - Lime Stabilized Lateritic Soil Blocks Subjected to Alternate Cycles of Wetting and Drying," *Civ. Environ. Eng.*, vol. 16, no. 1, pp. 30–38, 2020, doi: 10.2478/cee-2020-0004.
- [27] A. Kavak, G. Bilgen, and O. Faruk Capar, "Using Ground Granulated Blast Furnace Slag with Seawater as Soil Additives in Lime-Clay Stabilization," *J. ASTM Int.*, vol. 8, no. 7, pp. 1–12, 2011.
- [28] G. Bilgen, A. Kavak, and O. F. Capar, "Effect of steel slag used with sea water upon the strength of Uzunciftlik clay," in *Proceedings of the Third International Conference on New Developments in Soil Mechanics and Geotechnical Engineering*, 2012, pp. 693–700.
- [29] A. S. Muntohar and I. A. Khasanah, "Effect of moisture on the strength of stabilized clay with lime-rice husk ash and fibre against wetting-drying cycle," *Int. J. Integr. Eng.*, vol. 11, no. 9 Special Issue, pp. 100–109, 2019.





## Analysis of the seismic response of an RC frame structure with lead rubber bearings

Andrija Zorić<sup>\*1)</sup>, Dragan Zlatkov<sup>1)</sup>, Marina Trajković-Milenković<sup>1)</sup>, Todor Vacev<sup>1)</sup>, Žarko Petrović<sup>1)</sup>

<sup>1)</sup> University of Niš, Faculty of Civil Engineering and Architecture, 14 Aleksandra Medvedeva, 18000 Niš, Serbia

### Article history

Received: 27 December 2021

Received in revised form:

11 May 2022

Accepted: 15 May 2022

Available online: 30 June 2022

### Keywords

base isolation,  
lead rubber bearing,  
RC frame structure,  
El Centro,  
direct dynamic analysis

### ABSTRACT

Base isolation of buildings is the most efficient way of designing seismically resistant structures. Application of seismic isolators allows mutually independent movements of the ground and the structure during earthquakes. The application of seismic isolators increases the natural period of vibrations, which reduces the seismic forces in the structure. The paper analyzes the influence of the application of lead rubber bearings on the response of the structure to the action of an earthquake. A reinforced concrete frame structure was analyzed both for the case of base isolation and rigid foundation. Based on the comparative analysis of the natural period of vibrations, base shear seismic forces, displacement of the top level of the structure and relative inter-storey drift, conclusions were drawn about the efficiency of application of this type of seismic isolator. The required amount of ductility of a structure, as well as damage to structural and non-structural elements, is greatly reduced by base isolation.

## 1 Introduction

The influences on the structure caused by an earthquake are quite often dominant in the design of structures in seismically active areas. During an earthquake, damage to the structural and non-structural elements can be caused, as well as the collapse of the structure. This leads to significant consequences, such as huge material costs or, potentially, to the loss of human lives, which are irretrievable. Therefore, the seismic protection of buildings became a very attractive field of research in the 20th and 21st centuries.

The beginning of the concept of the design of seismically resistant structures dates from the end of the 19th and the beginning of the 20th century, resulting in the registration of various patents within this field. The proposed solutions consisted of separating the structure and the foundation by the system of the balls in concave bearings [1], as well as by a layer of sand or talc [2]. Such a system provided relative ground movement with regard to the building, lowering seismic forces in the structure. Nowadays, this concept is known as base isolation.

The modern base isolation concept is based on the application of devices that are set in seismic dilatation. Seismic dilatation is constructed at the level of the foundation or above the stiff basement structure, so the structure is divided into isolated structures and substructures. Seismic isolation devices are stiff enough in the vertical direction to transfer the gravity load, but they are less stiff in the horizontal direction. As a result, the natural period of vibration of the isolated structure increases up to several times compared to the rigidly founded structure. By

increasing the natural period of vibration of the structure, the values of mass acceleration are decreased as well as the intensity of the seismic forces in the structure. The application of these devices changes the response of the structure during an earthquake. A rigidly founded structure is dominantly deformed by bending and shearing due to an earthquake, while in the case of the base isolation, the structure is moving predominantly translational. That is why the damage to the structural elements of the seismically isolated structures is smaller compared to conventional structures. The intensity of the seismic forces in the structure also depends on the characteristics of the foundation ground. Due to the increasing natural period of vibration of the structure, the intensity of the seismic forces is decreased, while in the case of the soft ground seismic forces are increased. The seismic isolation of a structure has the greatest effect on the structure with the shortest natural period of vibration, as in the case of a good foundation in the ground.

According to the way the horizontal flexibility is provided, seismic isolators can be divided into elastomeric, sliding, and combined bearings [3]. Elastomeric bearings provide seismic isolation of structures with the flexibility of the material used for their manufacture. Natural or synthetic rubber is used in the production of elastomeric bearings. According to the level of damping, elastomeric bearings can be: low-damping rubber bearings, lead-rubber bearings, and high-damping rubber bearings [4-7].

A lead rubber bearing (LRB) has been developed in order to increase the damping of elastomeric bearings and to reduce the displacement of the structure. It consists of steel

\* Corresponding author:

E-mail address: [andrija.zoric@gaf.ni.ac.rs](mailto:andrija.zoric@gaf.ni.ac.rs)

plates, rubber, steel shims, and a lead core in the central part (Figure 1). The lead core is dominantly deformed by shear, characterized by a relatively small yield strength (usually about 10 MPa). Due to the plastification of the lead core, seismic energy is absorbed, and the force-displacement dependence of this isolator can be idealized by a bilinear diagram [8, 9].

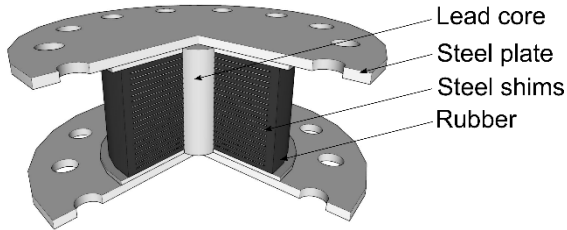


Figure 1. Characteristic section and basic parts of lead rubber bearing

Numerous experimental research has been conducted in order to determine the mechanical characteristics of this type of LRB. It has been confirmed that the lead core provides an adequate level of energy dissipation [4, 10-13]. The numerical models for the analysis of the properties of a LRB were also developed [12, 14-17]. The seismic analysis of base isolated structures confirmed that the use of LRB has a favourable effect on the structural response [18-20]. Similar results were confirmed in the analysis of the seismically isolated bridges [21].

The paper analyses the dynamic response of a reinforced concrete frame structure with LRB under the action of the north-south component of the Imperial Valley (El Centro) earthquake. A comparative study of the dynamic response of the structure was conducted with regard to the case of a rigidly founded structure. The analysis was performed on the SAP2000 software package.

## 2 Setting up the analysed problem

The effects of the application of base isolation of buildings are analysed on the reinforced concrete frame structure G<sub>r</sub>+13S<sub>t</sub>, with a storey height of 3 m. Frames are set at an equal distance of 4 m. The structure has 6 bays in

one and 4 bays in the other horizontal direction (Figure 2). The columns have a square cross-section of 60 cm, and the beams have a rectangular cross-section of b/h = 25/50 cm. The floor slabs are 20 cm thick. All structural elements are made of concrete, class C25/30. In both the lower and upper zones, the columns are reinforced with 12BØ20 and the beams with 5BØ16. The reinforcement was adopted so that the structure could bear both dead and live loads. The intensity of the dead load is 2.00 kN/m<sup>2</sup>, while the live load is 3.00 kN/m<sup>2</sup>. The loads are uniformly distributed over all floor slabs.

The analysis of the case when the structure is rigidly founded and supplied with base isolation with LRB is conducted. The LRB of the Dynamic Isolation System company is used. The maximum axial force in the columns under the serviceability load, which acts as a vertical force in the seismic isolator, is around 2300 kN. Based on the technical documentation, an isolator of 650 mm in diameter is adopted under each column, and its axial capacity is 2700 kN [22]. The isolator is composed of twenty layers of 12 mm thick rubber, and between each of them are 3 mm thick steel shims. In the central part of the isolator, a lead cylinder with a diameter of 150 mm is placed. The bilinear hysteretic behaviour of the isolator is described by elastic and post-elastic stiffness and yield strength. For the adopted isolator, the post-elastic stiffness is 505.3 kN/m and the yield strength is 100 kN. According to the manufacturer's recommendation, the horizontal elastic stiffness of the isolator is approximately 10 times larger than the post-elastic stiffness [22], and it is adopted in the paper. Analysis of the dynamic response of the structure under earthquake action also includes the influence of the vertical stiffness of the isolator, which is 700,000 kN/m [22].

## 3 Numerical analysis of the structure's seismic response

A numerical analysis of the structure's response during the earthquake was conducted in the software package SAP2000. The program is suitable for modelling 1D, 2D and 3D problems, including material and geometric nonlinearities, and analysing dynamically loaded structures using direct integration of equations of motion in the time domain.

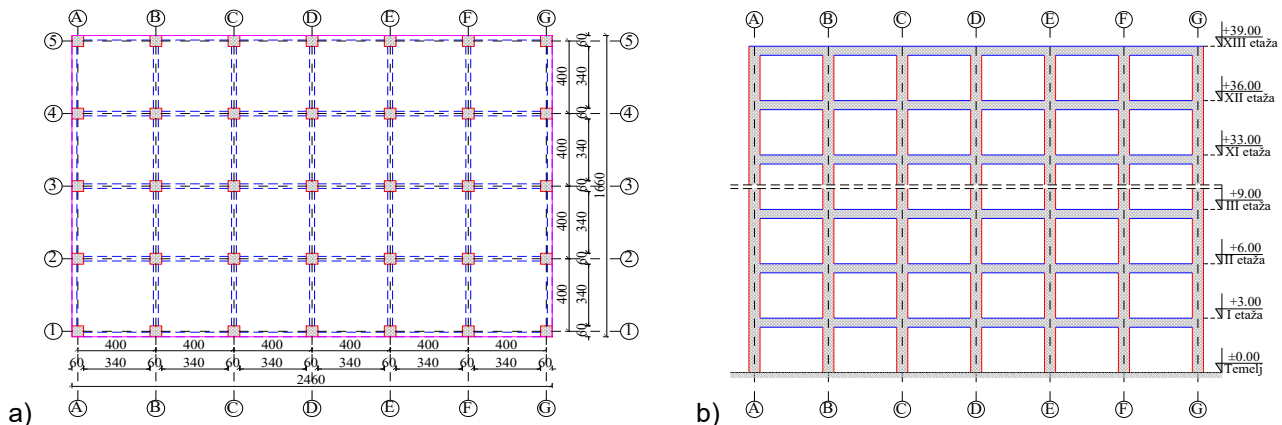


Figure 2. Disposition of the analysed structure; a) floor plan, b) longitudinal section

3.1 Finite element model

The geometry of the model is done in accordance with the geometry of the building (Figure 2). The columns and beams are modelled by 1D beam finite elements (FE), while floor structures are modelled with shell elements, where the appropriate geometric characteristics are defined. The length of the 1D finite elements is 1 m, while the floor structures are meshed with square finite elements with an edge length of 1 m. Relatively large dimensions of finite elements are adopted because of the complexity of the nonlinear calculation of the dynamic response of the structure by the method of direct integration of equations of motion. It did not significantly affect the accuracy of the results because the floor structures act as rigid diaphragms. The geometry of a numerical model with a finite element mesh is shown in Figure 3.

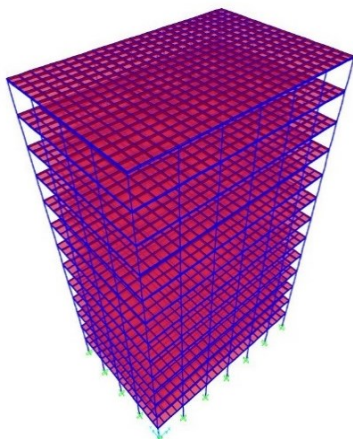


Figure 3. Geometry and FE mesh of the FEM model

Concrete is modelled as an isotropic material, whereby the modulus of elasticity is 31 GPa and the Poisson's ratio is 0.20. The Mander's stress-strain curve is adopted in order to describe the nonlinear behaviour of concrete, where the strain corresponding to the compressive strength of concrete is 2 ‰ and the ultimate strain is 5 ‰. Upon reaching the compressive strength, the material softens, and the slope of the stress-strain function is equal to 10 % of the modulus of elasticity (Figure 4a). In order to describe the hysteretic

behavior of the concrete, the Pivot model is adopted, which is recommended by software documentation and other researchers [23, 24]. The Pivot hysteresis model is defined by five parameters, which determine the reduction of stiffness due to the cyclic load. The parameters  $\alpha_1 = \alpha_2 = 1$ ,  $\beta_1 = \beta_2 = 0.30$ ,  $\eta = 10$  are adopted in the paper.

The stress-strain relationship (Figure 4b) is defined in order to describe the nonlinear behaviour of reinforced steel. The modulus of elasticity is 200 GPa and the yield strength is 500 MPa. After yielding, material hardening occurs up to the ultimate strain of 20 ‰, after which the material fails. In order to model the hysteretic behaviour of reinforcement under cyclic load, a kinematic model suitable for modelling ductile materials is adopted [23].

The characteristics of developing plastic hinges at the ends of beams and columns are defined with the purpose of covering the damage to the structure during an earthquake. Beams are dominantly loaded to bend about a horizontal central axis. Regarding that, the plastic hinges of beams are defined based on the bending moment. The moment-curvature relation in post-yielding behaviour depends on the cross-sectional dimensions, reinforcement ratio, and shear force. The yield curvature and post yield moment-curvature relation for beams are calculated based on the recommendations of FEMA-356 table 6-7 [25] for the adopted dimensions of cross-section and reinforcement of beams. Columns are dominantly loaded by axial force and bend about both horizontal central axes. Yield moment of columns depends on the intensity of axial force. The yield curvature and post yield moment-curvature relation for columns with interaction of axial force and bi-axial bending moments are defined in FEMA-356 table 6-8 [25]. Plastic deformations of column hinges are calculated according to these recommendations and adopted cross-sectional dimensions and reinforcement of columns.

In the case of the rigidly founded structure, the boundary conditions on the columns at ground-level are defined to prevent all translations and rotations. In the case of a base isolated structure, the modelling of seismic isolators is done using link elements with the definition of appropriate mechanical characteristics in three orthogonal directions. The isolator has linear elastic characteristics in the vertical direction and nonlinear bilinear behavior in the horizontal directions, where the corresponding characteristics are defined in accordance with the mechanical characteristics of the selected LRB (Section 2).

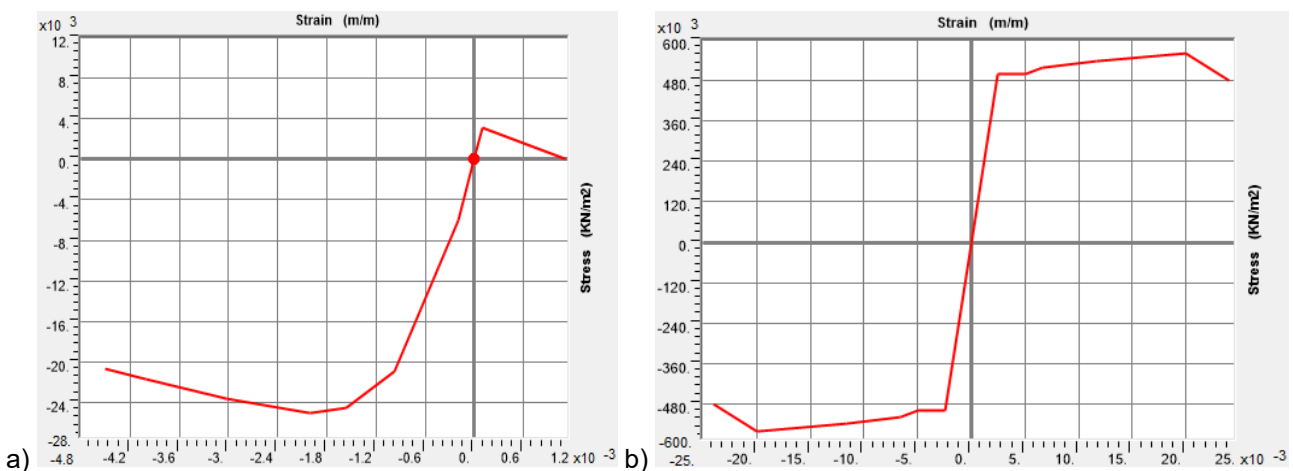


Figure 4. Stress-strain diagrams: a) concrete; b) reinforcement

In the dynamic analysis of models, the mass of the structure was defined as the sum of the dead and live load and the self-weight of the structure. A nonlinear static analysis of the structure for the combination of dead and live load is conducted. The nonlinear analysis includes material nonlinearity, while the P- $\Delta$  method models the geometric nonlinearity. P- $\Delta$  procedure is adequate in analyses in which the vertical load does not vary significantly. The stiffness matrix in the P- $\Delta$  procedure is constant during the calculation. This is considered as an advantage over the calculation methods that include large displacements where the stiffness matrix is calculated in each iteration step, because it requires less time for calculation.

The dynamic response of the structure to the action of the north-south component of the Imperial Valley earthquake is analysed. In the analysis, the earthquake load is defined as the acceleration of the supports in the x direction of the global coordinate system, using the earthquake accelerogram. The values of ground acceleration are defined in equal time intervals of 0.02 s, and the duration of the earthquake is 53.74 s (Figure 5).

The seismic response of the structure is calculated using direct integration of equations of motion in the time domain, which includes material and geometric nonlinearity via the P- $\Delta$  method. The dynamic calculation is conducted after the nonlinear static calculation for the combination of dead and live loads.

### 3.2 Model analysis parameters

Nonlinear dynamic analysis is conducted through 2687 sub-steps, with a time increment of 0.02 s, which corresponds to the discrete values of applied accelerogram of the Imperial Valley earthquake. The calculation includes the damping of 5 % defined by the Rayleigh model. The integration of the dynamic equations is performed by the implicit Hilber-Hughes-Taylor method, where the integration parameters are  $\alpha = 0$ ,  $\beta = 0.25$  and  $\gamma = 0.5$ .

The values of the natural periods of vibration, shear forces at the base, displacements of the top level of the building and relative inter storey drifts are considered in the comparative analysis of the dynamic responses of the

structure with and without LRB. Also, based on the plastic hinges propagation, a conclusion about the degree of structural damage is made. The economic aspect of the application of the seismic isolators is shown based on the required area of reinforcement in the columns in the case with and without LRB, designed for the action of dead and live load and the action of the Imperial Valley earthquake.

### 3.3 The results of the analysis and discussions

The basic dynamic parameter of each structure is the natural period of vibration. Therefore, it is set as a starting point for comparison of the structural response with and without LRB. Figure 6 and Figure 7 show the first three natural modes with the values of natural periods for a rigidly founded structure and a base isolated structure, respectively. It is noticed that with the application of LRB there is an increase in the natural period of vibration of the structure, i.e., to frequency reduction, which is one of the goals of the application of the seismic isolators. The increase in the period of oscillation occurs due to the deformability of the seismic isolators in the horizontal direction, so, unlike the rigidly supported structure, there are displacements of the supporting nodes. In comparison to the structure without seismic isolators, the natural periods of vibration of the structure with LRB are increased by 45 %. As the natural period increases, the acceleration of masses decreases along with the intensity of inertial forces during the earthquake.

The change in base shear force as a function of time is shown in Figure 8. With the application of LRB, the base shear force is reduced by about 50 %. In addition to the significant reduction in shear force due to the earthquake in the case of the base isolated structure, it should be noted that the change in shear force over time is more uniform than in the case of the rigidly founded structure. In the latter case, a sudden change in the ground acceleration is followed by the sudden oscillations of the shear force. The maximum value of the base shear force with and without LRB does not occur at the same time (Figure 8), which is a consequence of the longer natural period of the structure with LRB.

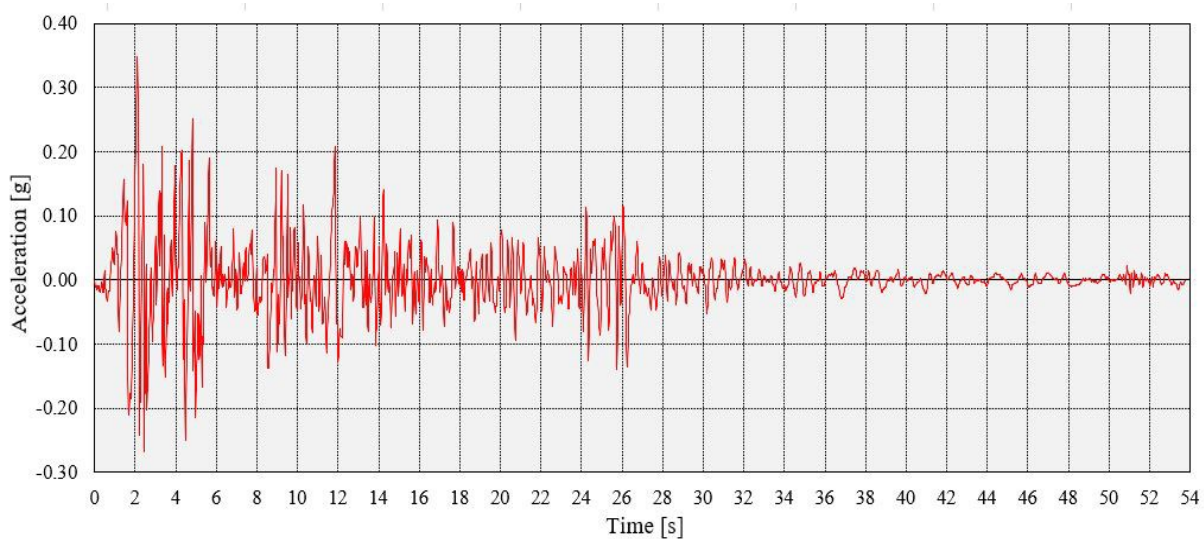


Figure 5. Accelerogram of Imperial Valley earthquake, component north-south

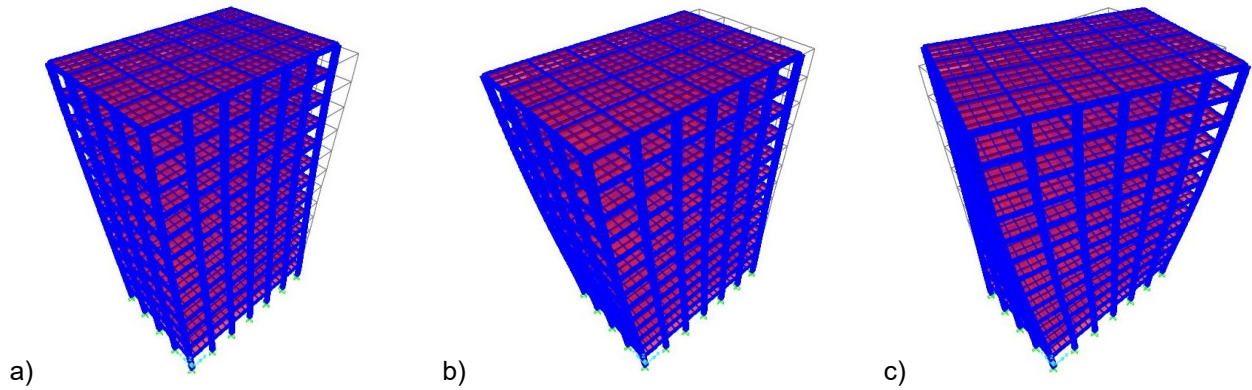


Figure 6. The first three mode shapes and natural periods of the rigidly founded structure: a) I period - y direction,  $T_1 = 1.395$  s; b) II period - x direction,  $T_2 = 1.343$  s; c) III period - torsion,  $T_3 = 1.203$  s

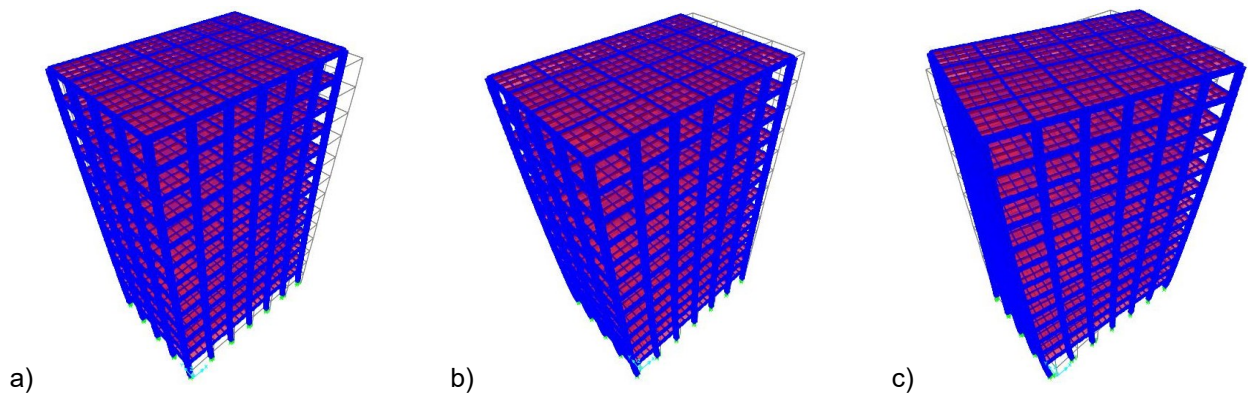


Figure 7. The first three mode shapes and natural periods of the base isolated structure: a) I period - y direction,  $T_1 = 2.044$  s; b) II period - x direction,  $T_2 = 1.981$  s; c) III period - torsion,  $T_3 = 1.759$  s

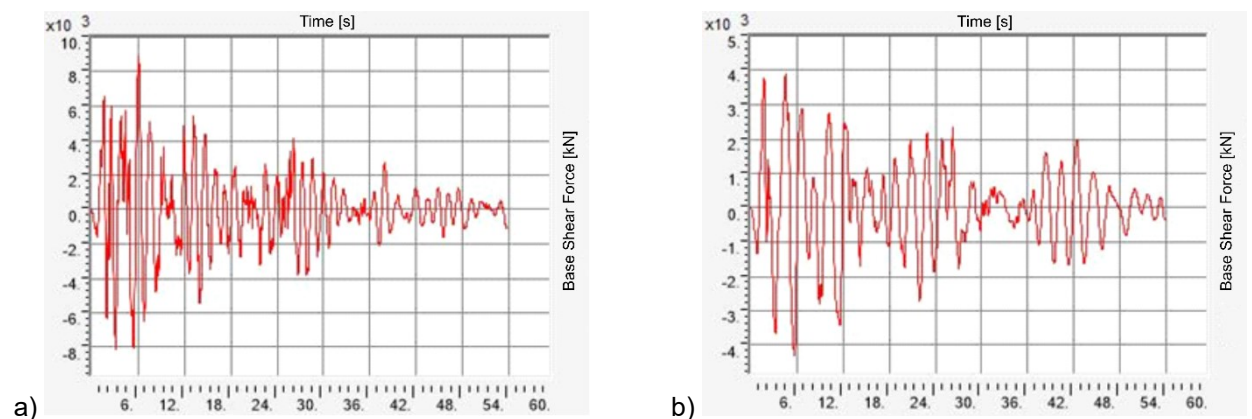


Figure 8. Base shear force vs. time, x direction: a) Rigidly founded structure, max 8909 kN at  $t = 6.00$  s; b) Base isolated structure, max 4303 kN at  $t = 5.68$  s

In Figure 9, the displacement of the top level of the structure with and without LRB as a function of time is presented. The displacement of the top level in the case with LRB is higher by about 35 % compared to the case without seismic isolators. Figure 10 shows the maximum horizontal displacements of the floors of the analysed models. Although the absolute displacement of the top of the structure with

LRB is larger than in the case without isolators, the fact that the supports displace too should be pointed out. The relative displacement of the top level of the structure with LRB in relation to the supports is 0.0663 m, which is about 35% less than the displacement of the top level of the rigidly founded structure.

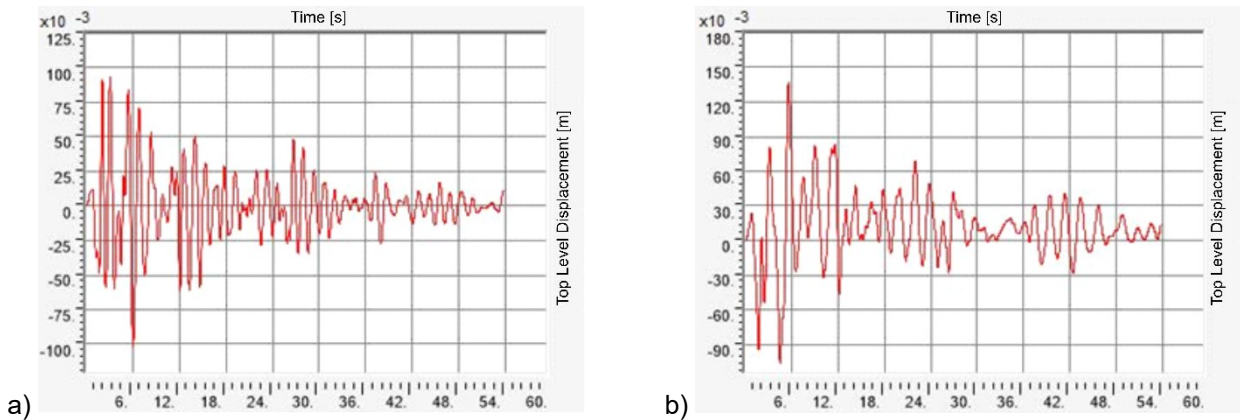


Figure 9. Horizontal displacement of top level of structure vs. time, x direction: a) Rigidly founded structure, max 0.1016 m at  $t = 6.04$  s; b) Base isolated structure, max 0.1373 m at  $t = 5.60$  s

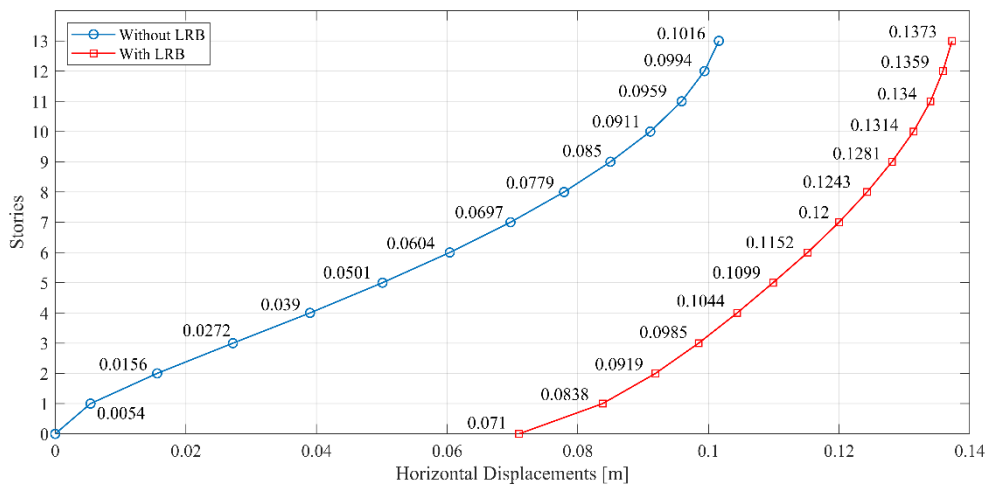


Figure 10. Maximum horizontal displacements of the floors in the earthquake directi

An important indicator of the response of the structure to the action of the earthquake is the relative interstorey drift. It is defined as the quotient of the divergence between the displacement of two adjacent floors and the storey height. Figure 11 shows the relative interstorey drifts of the structure

with and without LRB when the maximum displacement of the top level of the building is reached. The relative interstorey drifts in the case of the structure with LRB are smaller in relation to the case of rigidly supported structure for the 2<sup>nd</sup> floor and higher, while in the 1<sup>st</sup> floor it is larger.

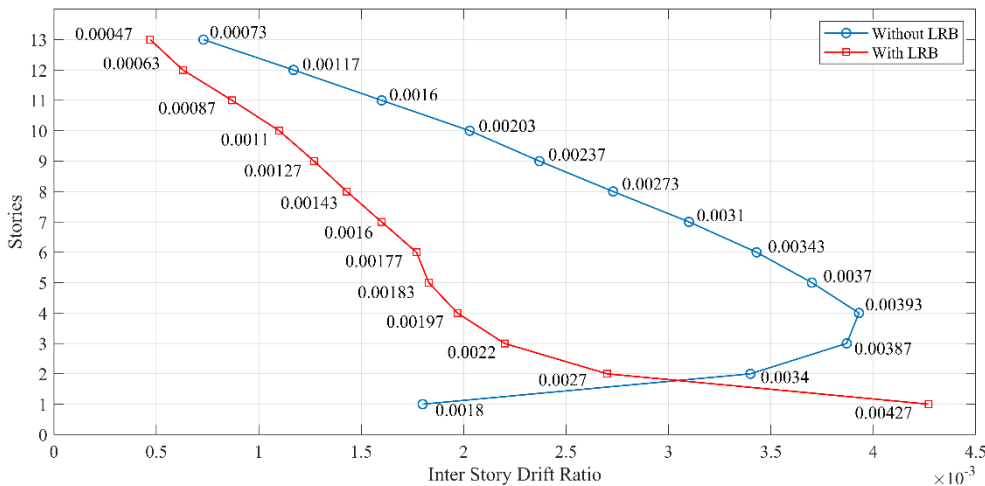


Figure 11. Interstorey drifts in the moment of maximum displacement of the top level of structure

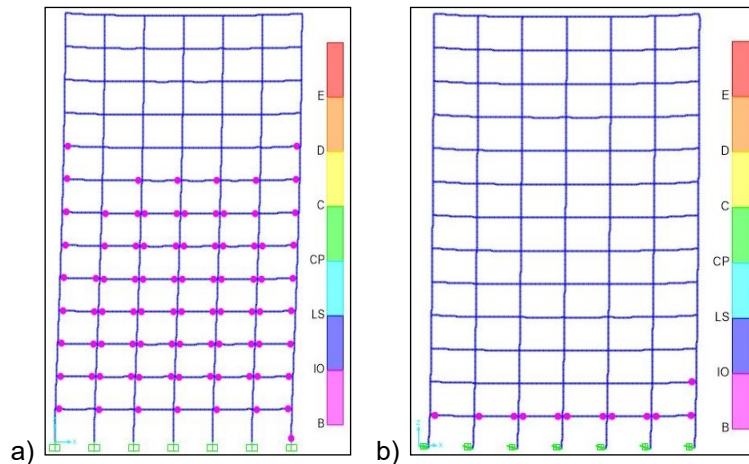


Figure 12. Plastic hinges in frame in the axis 3-3; a) rigidly founded structure; b) base isolated structure

According to the analysis of plastic deformations of the beam and column joints, it can be observed that the beam joint plastification occurs both in the model without and with LRB (Figure 12). In the case of the building without LRB the ends of all beams up to the 8th floor are plastificated, as well as the joints of individual columns, while in the case of a building with seismic isolators, the ends of all beams up to the first floor are plastificated. This is considered to be the consequence of lower seismic force in the case of the application of LRB, and of dissipation of the part of the seismic energy by plastic deformations of the lead core. The maximum plastic rotation in a model without LRB is 0.002559 rad, while by the application of LRB, maximum plastic rotation is decreased to 0.001318 rad. The application of lead rubber bearings significantly reduces the plastic deformations of the structure, which results in less damage to the structure during the earthquake compared to damage of the non-isolated structure.

The design of all columns for the effects of dead and live load and seismic action was conducted in accordance with Eurocodes 2 and 8 [26, 27]. The design of the columns was conducted in order to compare the required area of reinforcement in the columns in the model without and with LRB. In the case of the model without LRB, the maximum required area of reinforcement is 70,5 cm<sup>2</sup>, while in the model with LRB it is 44,9 cm<sup>2</sup>. The reduction of the seismic forces in the structure with seismic isolators is reflected in the reduction of the required area of reinforcement in the columns by 36%.

#### 4 Conclusion

Based on the results of the numerical analyses conducted in this work, the following conclusions can be drawn:

- the application of the lead rubber bearings increases the natural periods of vibration of the analysed structure by approximately 45%,
- the application of lead rubber bearings significantly improves the dynamic response of the structure, which is reflected in a significant reduction of seismic forces, displacement of the top level of the structure and relative inter storey drifts,
- the application of lead rubber bearings reduces the development of plastic hinges in beams and columns compared to the rigidly founded structure, which is an

especially important advantage because the occurrence of plastic hinges in columns can lead to the loss of bearing capacity and stability of the entire structure,

- lead rubber bearings contribute to the reduction of the influences in the structural elements, which results in the reduction of the required area of reinforcement in the RC columns.

Further research in this area should be focused on parametric analysis of the dynamic response of structures during earthquakes, varying the stiffness of the LRB. The structure analysed in this paper is regular in plan and elevation, so further research can be directed towards analysing the effects of LRB application in structures with irregularities.

#### Acknowledgements

The research is supported by the Serbian Ministry of Education, Science and Technological Development through the TR 36016 project.

#### References

- [1] J. Touaillon, Improvement in buildings, United States of America Patent No. 99,973, Feb. 15. 1870.
- [2] J.A. Calantarients, Building construction to resist the action of earthquake, United States of America Patent No. 932,443, Aug. 31. 1909.
- [3] T.E. Saaed, G. Nikolakopoulos, J.-E. Jonasson, H. Hedlung, State of the Art of Structural Control, J. Vib. Control. 21(5) (2015) 919-937.
- [4] J.M. Kelly, Aseismic base isolation: review and bibliography, Soil Dyn. Earthq. Eng. 5(3) (1986) 202-216.
- [5] F. Naeim, J.M. Kelly, Design of seismic isolated structures: from theory to practice, John Wiley & Sons, New York, 1999.
- [6] M. Higashino, S. Okamoto, Response Control and Seismic Isolation of Buildings, Taylor & Francis, London, 2006.
- [7] G.P. Warn, K.L. Ryan, A Review of Seismic Isolation for Buildings: Historical Development and Research Needs, Buildings, 2(3) (2012) 300-325.
- [8] W.H. Robinson, A.G. Tucker, A Lead-Rubber Shear Damper, Bull. N. Z. Soc. Earthq. Eng. 10(3) (1977) 151-153.

- [9] W.H. Robinson, Lead-Rubber Hysteretic Bearings Suitable for Protecting Structures during Earthquake, *Earthq. Eng. Struct. Dyn.* 10(4) (1982) 593-604.
- [10] G.P. Warn, A.S. Whittaker, A Study of the Coupled Horizontal-Vertical Behavior of Elastomeric and Lead-Rubber Seismic Isolation Bearings, Report No. MCEER-06-0011, University of Buffalo, New York, USA, 2006.
- [11] G.P. Warn, A.S. Whittaker, M.C. Constantinou, Vertical Stiffness of Elastomeric and Lead-Rubber Seismic Isolation Bearings, *J. Struct. Eng.* 133(9) (2007) 1227-1236.
- [12] S. Eem, D. Hahm, Large strain nonlinear model of lead rubber bearings for beyond design basis earthquakes, *Nucl. Eng. Technol.* 51(2) (2019) 600-606.
- [13] G.-H. Koo, T.-M. Shin, S.-J. Ma, Shaking Table Tests of Lead Inserted Small-Sized Laminated Rubber Bearing for Nuclear Component Seismic Isolation, *Appl. Sci.* 11(10) (2021) 1-17.
- [14] Y.-f. Wu, H. Wang, A.-q. Li, D.-m. Feng, B. Sha, Y.-p. Yhang, Explicit finite element analysis and experimental verification of a sliding lead rubber bearing, *J. Yhejiang Univ. Sci. A*, 18(5) (2017) 363-376.
- [15] M. Saedniya, S.B. Talaeitaba, Numerical modeling of elastomeric seismic isolators for determining force-displacement curve from cyclic loading, *Int. J. Adv. Struct. Eng.* 11(3) (2019) 361-376.
- [16] M. Trajković-Milenković, O.T. Bruhns, A. Zorić, On instability of constitutive models for isotropic elastic-perfectly plastic material behaviour at finite deformations, *J. Mech. Eng. Sci. OnlineFirst* (2020) 1-12.
- [17] A. Khaloo, A. Maghsoudi-Barmi, M.E. Moeini, Numerical parametric investigation of hysteretic behavior of steel-reinforced elastomeric bearings under large shear deformation, *Structures*, 26 (2020) 456-470.
- [18] Y.-S. Choun, J. Park, I.-K. Choi, Effects of Mechanical Property Variability in Lead Rubber Bearings on the Response of Seismic Isolation System for Different Ground Motions, *Nucl. Eng. Technol.* 46(5) (2014) 605-618.
- [19] V.-T. Nguyen, X.-D. Nguyen, Seismic response of multi-story building isolated by Lead-Rubber Bearings considering effects of the vertical stiffness and buckling behaviors, VII International Scientific Conference "Integration, Partnership and Innovation in Construction Science and Education, IOP Conference Series: Material Science and Engineering, Tashkent, Uzbekistan, 2020.
- [20] S.-H. Ju, C.-C. Yuantien, W.-K. Hsieh, Study of Lead Rubber Bearing for Vibration Reduction in High-Tech Factories, *Appl. Sci.* 10(4) (2020) 1-17.
- [21] N. Shaban, A. Caner, Shake table tests of a different seismic isolation systems on a large scale structure subjected to low to moderate earthquakes, *J. Traffic Transp. Eng.* 5(6) (2018) 480-490.
- [22] Dynamic isolation Systems, <http://www.dis-inc.com/technical.html>, (accessed 9 August 2021).
- [23] CSI Analysis Reference Manual, Computers and Structures Inc., Berkley, California, USA, 2016.
- [24] D. Cardone, A. Flora, G. Gesualdi, Inelastic response of RC frame building with seismic isolation, *Earthq. Eng. Struct. Dyn.* 42(6) (2013) 871-889.
- [25] FEMA 356 Prestandard and Commentary for the Seismic Rehabilitation of Buildings, American Society of Civil Engineers, Washington, D.C., USA, 2000.
- [26] EN 1992-1-1:2015, Eurocode 2, Design of concrete structures – Part 1-1: General rules and rules for buildings, Brussels, 2015.
- [27] EN 1998-1:2015, Eurocode 8, Design of structures for earthquake resistance – Part 1: General rules, seismic actions and rules for buildings, Brussels, 2018.

## INSTRUCTIONS FOR AUTHORS

### Acceptance and types of contributions

The Building Materials and Structures journal will publish unpublished papers, articles and conference reports with modifications in the field of Civil Engineering and similar areas (Geodesy and Architecture). The following types of contributions will be published: original scientific papers, preliminary reports, review papers, professional papers, objects describe / presentations and experiences (case studies), as well as discussions on published papers.

Original scientific paper is the primary source of scientific information and new ideas and insights as a result of original research using appropriate scientific methods. The achieved results are presented briefly, but in a way to enable proficient readers to assess the results of experimental or theoretical numerical analyses, so that the research can be repeated and yield with the same or results within the limits of tolerable deviations, as stated in the paper.

Preliminary report contains the first short notifications on the results of research but without detailed explanation, i.e. it is shorter than the original scientific paper.

Review paper is a scientific work that presents the state of science in a particular area as a result of analysis, review and comments, and conclusions of published papers, on which the necessary data are presented clearly and critically, including the own papers. Any reference units used in the analysis of the topic are indicated, as well as papers that may contribute to the results of further research. If the reference data are methodically systematized, but not analyzed and discussed, such review papers are classified as technical papers.

Technical paper is a useful contribution which outlines the known insights that contribute to the dissemination of knowledge and adaptation of the results of original research to the needs of theory and practice.

Other contributions are presentations of objects, i.e. their structures and experiences (examples) in the construction and application of various materials (case studies).

In order to speed up the acceptance of papers for publication, authors need to take into account the Instructions for the preparation of papers which can be found in the text below.

### Instructions for writing manuscripts

The manuscript should be typed one-sided on A-4 sheets with margins of 31 mm (top and bottom) and 20 mm (left and right) in Word, font Arial 12 pt. The entire paper should be submitted also in electronic format to e-mail address provided here, or on CD. The author is obliged to keep one copy of the manuscript.

As of issue 1/2010, in line with the decision of the Management Board of the Society and the Board of Editors, papers with positive reviews, accepted for publication, will be published in Serbian and English, and in English for foreign authors (except for authors coming from the Serbian and Croatian speaking area).

Each page should be numbered, and the optimal length of the paper in one language is about 16 pages (30.000 characters) including pictures, images, tables and references. Larger scale works require the approval of the Board of Editors.

The title should describe the content of the paper using a few words (preferably eight, and up to eleven). Ab-

brevisions and formulas should be omitted in the title. The name and surname of the author should be provided after the title of the paper, while authors' title and position, as well as affiliation in the footnote. The author should provide his/her phone number, e-mail address and mailing address.

The abstract (summary) of about 150-250 words in Serbian and English should be followed by key words (up to seven). This is a concise presentation of the entire article and provides the readers with insight into the essential elements of the paper.

The manuscript is divided into chapters and sub-chapters, which are hierarchically numbered with Arabic numerals. The paper consists of introduction and content with results, analysis and conclusions. The paper ends with the list of references. All dimensional units must be presented in international SI measurement units. The formulas and equations should be written carefully taking into account the indexes and exponents. Symbols in formulas should be defined in the order they appear, or alternatively, symbols may be explained in a specific list in the appendix. Illustrations (tables, charts, diagrams and photos) should be in black and white, in a format that enables them to remain clear and legible when downscaled for printing: one to two columns (8 cm or 16.5 cm) in height, and maximum of 24.5 cm high, i.e. the size of the letters and numbers should be at least 1.5 mm. Original drawings should be of high quality and fully prepared for copying. They also can be high-quality, sharp and contrasting photo-copies. Photos should be in black and white, on quality paper with sharp contours, which enable clear reproduction.

The list of references provided at the end of the paper should contain only papers mentioned in the text. The cited papers should be presented in alphabetical order of the authors' first name. References in the text should be numbered with Arabic numerals in square brackets, as provided in the list of references, e.g. [1]. Each citation in the text must be contained in the list of references and vice versa, each entry from the list of references must be cited in the text.

Entries in the list of references contain the author's last name and initials of his first name, followed by the full title of the cited article, the name of the journal, year of publication and the initial and final pages cited (from - to). If the doi code exists it is necessary to enter it in the references. For books, the title should be followed by the name of the editor (if any), the number of issue, the first and last pages of the book's chapter or part, the name of the publisher and the place of publication, if there are several cities, only the first in the order should be provided. When the cited information is not taken from the original work, but found in some other source, the citation should be added, "cited after ..."

Authors are responsible for the content presented and must themselves provide any necessary consent for specific information and illustrations used in the work to be published.

If the manuscript is accepted for publication, the authors shall implement all the corrections and improvements to the text and illustrations as instructed by the Editor.

Writings and illustrations contained in published papers will not be returned. All explanations and instructions can be obtained from the Board of Editors.

Contributions can be submitted to the following e-mails: [sneska@imk.grf.bg.ac.rs](mailto:sneska@imk.grf.bg.ac.rs) or [miram@uns.ac.rs](mailto:miram@uns.ac.rs)  
Website of the Society and the journal: [www.dimk.rs](http://www.dimk.rs)

Financial support



**MINISTRY OF EDUCATION, SCIENCE AND  
TECHNOLOGICAL DEVELOPMENT OF  
REPUBLIC OF SERBIA**



**UNIVERSITY OF BELGRADE FACULTY OF  
CIVIL ENGINEERING**



**INSTITUTE FOR TESTING OF MATERIALS-  
IMS INSTITUTE, BELGRADE**



**FACULTY OF TECHNICAL SCIENCES,  
UNIVERSITY OF NOVI SAD, DEPARTMENT  
OF CIVIL ENGINEERING**



**ИНЖЕЊЕРСКА  
КОМОРА  
СРБИЈЕ**

**SERBIAN CHAMBER OF ENGINEERS**